2014-10-02

Power Amplifier Behavioral Modeling Algorithms for Digital/Hybrid Predistortion in Software Defined Transmitters

Rawat, Piyush

UNIVERSITY OF CALGARY

Power Amplifier Behavioral Modeling Algorithms for Digital/Hybrid Predistortion in Software Defined Transmitters

by

Piyush Rawat

A THESIS

SUBMITTED TO THE FACULTY OF GRADUATE STUDIES

IN PARTIAL FULFILMENT OF THE REQUIREMENTS FOR THE

DEGREE OF MASTER OF SCIENCE

GRADUATE PROGRAM IN ELECTRICAL AND COMPUTER ENGINEERING

CALGARY, ALBERTA

SEPTEMBER, 2014

Abstract

Power amplifier (PA) is a vital component of transmission system and effect of PA nonlinearity and memory effects are generally investigated in system level analysis of communication systems. Among time and frequency domain approaches, time domain behavioral modeling is more popular as it also considers memory effect and it finds useful application as inverse modeling for digital predistorter to enhance the signal quality. Among many models, Memory polynomial (MP) model is still considered as most simple and effective parametric model as it provides best modeling performance with less complexity.

This thesis investigates two models, which aim to improve stability and accuracy of memory polynomial model. The proposed Pseudo Zernike Memory polynomial (PZMP) model is modified version of the Zernike polynomial function, which provides more robust performance in terms of better condition number and dispersion coefficients for PA behavioral modelling, with respect to previously proposed models such as orthogonal memory polynomial (OMP) and MP model. It provides approximately,

i) . 75% and 50% improvement in terms of dispersion coefficients (in dB) over MP model and OMP model respectively; ii). 61% and 15% improvement in terms of condition number (in dB) over MP model and OMP model respectively.

The other model takes advantage of recursive property of Rational Polynomial (RP), which is closer to the physical analogy of PA. The proposed model retrieves data in two steps to maintain causality of the system. The proposed two-step-rational polynomial model improves modeling performance in terms of in-band and out-of-band performance and provides far better modeling as compared to memory polynomial model.

This thesis also includes the study of hydrid digital predistortion (DPD) technique for complete RF-in and RF-out system. The system is implemented in Field-Programmable Gate (FPGA) using Look-Up Tables (LUT). The compensation of the *I-Q* (Inphase-Quadrature phase) imbalance in the setup is further studied for such system.

Acknowledgements

I would like to express my sincere gratitude to my supervisor, Professor Dr. Fadhel M. Ghannouchi for giving me the opportunity to pursue my MSc degree under his supervision. This thesis could not exist without your guidance and encouragement. Thank you for your gracious support and insight and for providing me with this opportunity to explore my interests in the field of predistortion.

I would also like to thank all the wonderful and diverse members and all my colleagues in iRadio lab group, especially Dr. Mohamed Helaoui, Dr. Meenakshi Rawat, Dr. Karun Rawat and my colleague Andrew Kwan from whom I get fruitful insights of the project, which helped me a lot throughout my research. To the administrative staff at the Electrical Engineering Department, thank you for all your hard work behind the scenes and making my research possible. To my parents, thank you for instilling in me a love for engineering and natural sciences. Thank your also for your continued support and encouragement through the many years that led up to the completion of my thesis.

To my Sister and my Brother-in-law

To my parents Mrs. Laxmi Rawat and Mr. Sunder Singh Rawat

To my Brothers Dr. Pradeep Singh Rawat and Abhishek Rawat

To my sister-in-law Shivani Aswal Rawat

To my cousin Meghna Gautam and my friends

Table of Contents

Abstract i
Acknowledgements iii
Table of Contents v
List of Tables vii
List of Figures and Illustrations viii
List of Symbols, Abbreviations and Nomenclature x

CHAPTER ONE: INTRODUCTION 1
1.1 Motivation 1
1.2 Power Amplifier Linearization Techniques 2
1.3 Pre-distortion Techniques 5
1.4 Problem Definition and Targeted Goals 10
1.5 Statement of Objectives 10
1.6 Thesis Outline 11

CHAPTER TWO: PSEUDO-ZERNIKE POLYNOMIALS FOR NUMERICALLY STABLE PA MODELING USING 3G+ SIGNALS 13
2.1 Introduction 13
2.2 Pseudo-Zernike Memory Polynomial Model 14
2.3 Pseudo-Zernike Polynomial Model Performance in the presence of Non-Uniform Signal Pdfs 17
2.3.1 Observation Matrix Performance 19
2.4 Model Performance of Different Polynomial Models for 3G+ Signals 20
2.5 Conclusion 27

CHAPTER THREE: RATIONAL FUNCTION BASED TWO-STEP MODEL FOR ACCURATE MODELING AND DPD FOR HIGH POWER AMPLIFIERS 28
3.1 Introduction 28
3.2 State-of-the-art memory polynomial model 29
3.3 Rational function model 30
3.4 Two-step RF model description 32
3.5 Measurement Setup 34
3.6 Modeling Performance 36
3.7 Conclusion 40

CHAPTER FOUR: HYBRID RF-DIGITAL PREDISTORTION SYSTEM 41
4.1 Introduction 41
4.2 Background and design of Hybrid RF-PD System 42
4.3 System Description 43
4.3.1 PA Characterization 45
4.3.2 PD implementation 47
4.4 I-Q imbalance Calibration 50
4.5 Vector Multiplier characterization for I-Q imperfection 53
4.6 Envelope Memory Polynomial for memory effect inclusion 57

4.7 Conclusion 60

CHAPTER FIVE: SUMMARY AND FUTURE PLANS 61
5.1 Summary 61
5.2 Key Points for Future Developments 62

REFERENCES 63

List of Tables

Table 2.1 Condition No. (in dB) for 3G+ Signals 22

Table 2.2 Dispersion Coefficients (in dB) for 3G+ Signals 23

Table 3.1 Comparison between MPM and RPM with different 3G+ signals for Class AB Amplifier..... 37

Table 4.1 Different cases in the characterization of the RF vector multiplier in the hybrid RF-DPD system 54

Table 4.2 Measured ACLR summary of various conditions for one- and three-carrier WCDMA signals..... 57

List of Figures and Illustrations

Figure 1.1 PA linearization Techniques (a) Feed-Forward Technique, (b) Feed-Back Technique with Amplifier gain A and Feedback β, (c) Predistortion Technique 3

Figure 1.2 Post-Distortion Technique 6

Figure 1.3 Predistortion Scheme. (a) Analog predistortion (b) Digital predistortion (c) Hybrid RF-digital -predistortion, (d) Predistortion operation. 7

Figure 1.4 Non-linear phase compression characteristic (AM-AM) and its correction. 9

Figure 1.5 Non-linear phase compression characteristic (AM-PM) and its correction. 9

Figure 2.1 Histogram's of Input signals having different distribution functions. 18

Figure 2.2 Condition Number (in dB) of observation matrix for OMP as well as PZMP for memory less case 20

Figure 2.3 Probability density functions of different signals 21

Figure 2.4 Comparison of ACEPR Performances 25

Figure 2.5 Comparison of NMSE Performances 26

Figure 3.1 Signal distortion and resultant spectrum re-growth due to PA Non-linearity. 28

Figure 3.2 Block-wise description of two-step rational function model 33

Figure 3.3 Measurement setup for the DPD using Class AB Power Amplifier 35

Figure 3.4 Spectrum of WCDMA_111 signal input (black), spectrum of the modeling error for MP (blue) and RP (red) Models 38

Figure 3.5 Spectrum of WCDMA_1001 signal input (black), spectrum of the modeling error for MP (blue) and RP (red) Models 38

Figure 3.6 Spectrum of WCDMA_1111 signal input (black), spectrum of the modeling error for MP (blue) and RP (red) Models 39

Figure 4.1 Hybrid DPD Technique implementation scheme. 43

Figure 4.2 Block diagram of the hybrid RF-DPD system. 44

Figure 4.3 Setup for characterizing the power amplifier to obtain its nonlinear characteristics in terms of AM-AM and AM-PM responses. 46

Figure 4.4 Vector decomposition of the predistorter complex gain characteristic for generating LUT entries corresponding to the control voltages of the RF vector multiplier with no I-Q imperfection. 47

Figure 4.5 Linear response of logarithmic detector based on its characterization..... 50

Figure 4.6 Vector decomposition of the predistorter complex gain characteristic for generating LUT entries corresponding to the control voltages. 51

Figure 4.7 Setup for characterizing the RF vector multiplier for I-Q imperfection in the hybrid RF-DPD system. 53

Figure 4.8 Absolute phase measurement of different cases in RF vector multiplier characterization. 55

Figure 4.9 Detailed block diagram of EMP model 58

Figure 4.10 Measured output spectrum of the PA for one-carrier WCDMA signal..... 59

List of Symbols, Abbreviations and Nomenclature

Symbol	Definition
ACEPR	Adjacent Channel Error Power Ratio
ACPR	Adjacent Channel Power Ratio
ACLR	Adjacent Channel Leakage Power Ratio
AM-AM	Amplitude Modulation to Amplitude Modulation
AM-PM	Amplitude modulation to Phase modulation
DAC	Digital-To-Analog Converters
DPD	Digital predistortion
DSP	Digital Signal Processor
DVB-T	Digital Video Broadcasting-Terrestrial
EDET	Envelope Detector
EFB	Envelope feedback
EPA	Error Power Amplifier
EPSD	Error Power Spectrum Densities
FB	Feedback
FF	Feedforward
FPGA	Field Programmable Gate Array
GHz	Gigahertz
I	In-phase
IMD	Inter-modulation Distortion
LS	Least Squares
LUT	Look-Up Table
MHz	Megahertz
MIF	Memory Initialization Files
MP	Memory Polynomial
NMSE	Normalized Mean Square Error
OMP	Orthogonal Memory Polynomial
PA	Power Amplifier
PAPR	Peak-Average-to-Power Ratio
PD	Predistortion
PDF	Probability Density Function
PZMP	Pseudo Zernike Memory Polynomial
Q	Quadrature-phase
RAM	Random Access Memory
RF	Radio frequency
RF-DPD	Radio Frequency digital predistortion
RP	Rational Polynomial
RPM	Rational Polynomial Model
SVD	Singular Value Decomposition
VNA	Vector NetworkAanalyzer
VSA	Vector Spectrum Analyzer
VSG	Vector Signal Generator

WCDMA	Wide-band Coded Multiple Access
Wi-MAX	Worldwide Interoperability for Microwave Access
ZMP	Zernike Memory Polynomial
2G	Second Generation
3G	Third Generation
3G+	Third Generation and beyond Signals

Chapter One: Introduction

In the world of fast growing technology, the mode of communication holds the significant importance, which makes the wireless communication an immensely important and common feature of everyday life. To pace up the ever expanding need of modern technology and fulfil the challenges to get an efficient and most reliable wireless system, a lot of research and innovations has been carried out in various areas in communication engineering. A publication in *Library of Parliament Research* confirms the incredible increase in the wireless technology (like mobile cell phone and wireless transmission) usage in Canada and almost triple data usage on worldwide scale in past few years [1], [2], [3]. The recent studies depict the tremendous increase in data usage in Canada itself in upcoming 5 years [4]. Obviously, the exponentially increasing demand of data usage for ideal wireless communication makes it one of the most important and vast areas of research. This ensure the goals of modern wireless standards say third-generation beyond (3G+) signals to provide the high data rates to the end user in order to meet the requirements of broadband services of users while maintaining the quality of service even when migrating from second-generation (2G) to third-generation (3G) and higher standards. The demand of high data rates, high spectral efficiency leads to the origin of upcoming wireless standards like Wide-band Coded Multiple Access (WCDMA) [5], Worldwide Interoperability for Microwave Access (WiMAX)[6], Digital Video Broadcasting (DVB)[7] and Long Term Evolution (LTE)[8] to meet up the new challenges, as a result of continuous development and emergence of new protocols.

1.1 Motivation

Due to considerable development and vast scope of wireless communication nowadays, the stable and accurate transmission also plays a key role. The accurate transmission signifies the better in-

band [10] and out-of-band [10] performances and less complexity [10] in transmission system. The transmission system comprises of a complex system in which, Power Amplifier (PA) is the most vital component that is non-linear in nature. There has been a lot of interest in its behavioral modeling to be used in the system level analysis of wireless signals and thus communication systems. There are two main approaches for PA modeling, time domain and frequency domain approach. The time domain behavioral modelling is vastly used and is more popular as it explicitly considers memory effects [9]. Moreover, once an accurate model is derived it can be easily applied as inverse modeling for digital predistorter, which is discussed in detail in section 1.4.

The motivation mainly here is,

1. To improve the in-band [10] and out-of-band [10] distortion characteristic modeling while using 3G+ signals using most appropriate memory polynomial model, which ensures better performance even at high non-linear order, and therefore will lead to more accurate output after predistortion.
2. To improve the numerical stability when identifying the models used for PA modeling.

The two figures of merits, the condition number [10] and dispersion coefficient [10] has direct impact on modeling identification stability of PAs. It is established in literature that when model observation matrices are better conditioned and coefficients are less dispersed, they provide much better performances in fixed-point calculation scenario [11].

1.2 Power Amplifier Linearization Techniques

The modern communication system applications, several techniques have been proposed for power amplifier linearization. These techniques can be roughly classified into three groups: feedforward

(FF) [14], feedback (FB) [15-[16] and predistortion (PD) [13] as shown in Figure 1.1 (a), 1.1(b), and 1.1(c), respectively.

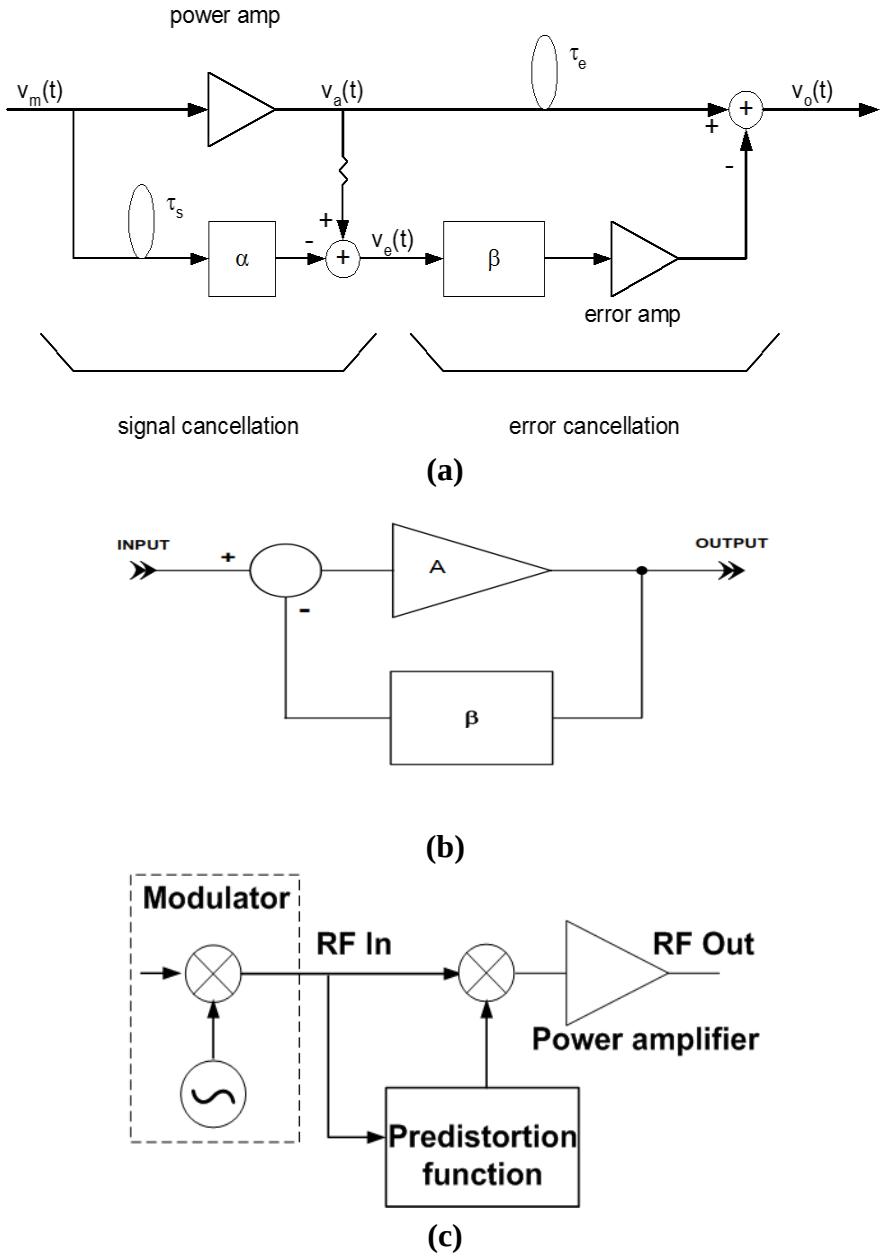

Figure 1.1 PA linearization Techniques (a) Feed-Forward Technique, (b) Feed-Back Technique with Amplifier gain A and Feedback β, (c) Predistortion Technique

The FF technique is the most popular PA linearization technique for a base station application because of its outstanding performance in inter-modulation distortion (IMD) correction [17]. The FF technique is devised by, Harold S. Black, who is also recognized as the inventor of the FB technique in 1928 [18]. His basic idea for the FF technique was to build two identical amplifiers and use one amplifier to subtract the distortion from the other; however, the power capacity of the error power amplifier (EPA) used in modern FF systems is often from 10 percent to 25 percent of the saturation power of the main amplifier. The output of the main amplifier feeds a perfectly linear attenuator for IMD estimation. The attenuated output is then subtracted from the input to yield a signal that is a perfectly scaled version of the distortion. This pure distortion signal feeds the EPA. The distortion signal from the EPA is subtracted from the distorted signal of the main amplifier to yield a final output that greatly reduces distortion. Since no feedback is involved, it is free from stability issue as in FB type linearization. Moreover, it does not reduce amplifier gain. Changes of device characteristics with time and temperature are not corrected because of its open-loop nature. Therefore, an adaptive control method is essential in FF linearization [14].

Although the adaptive control methods are employed, it is not easy to simultaneously maintain both amplitude and phase over the correction bandwidth of such a high degree. Furthermore, an error amplifier, a delay line and combiners are required at the output of the main PA to compensate for the IMDs and cause a large amount of insertion loss and circuit complexity, ultimately leading to poor efficiency.

The FB technique is one of the simplest techniques for reducing amplifier distortion. The inventor of FF technique, Harold S. Black invented a negative FB technique as a way to solve the distortion problem of positive FB [19-20]. The simplest negative FB technique applied to radio frequency (RF) amplifiers is RF FB. Since RF amplifiers display much larger phase shifts and electrical

length at gigahertz frequencies, the electrical delays around the FB loop restrict the bandwidth of signals that can be linearized. To eliminate the drawback of group delay problems in the RF FB techniques, envelope feedback (EFB) techniques that use envelope amplitude and phase variations offer some potential for bypassing fundamental phase-delay problems. [15-16]. Still, the principal limitation of FB techniques is the inability to handle wideband signals. In practice, it is difficult to make a FB system respond to signal-envelope changes much greater than several MHz, due to the delay of the amplifier and associated signal-processing components.

PD [13] involves the creation of a distortion characteristic that is precisely opposite to the distortion characteristic of the RF PA, where the cascade of the two ensures that the resulting system has little or no input-output distortion. Since linearization is performed at the input of the PA, loss of efficiency is negligible. This thesis revolves around concept and requirements of modeling for pre-distortion techniques.

1.3 Pre-distortion Techniques

PD is theoretically the simplest form of linearization for an RF power amplifier because of its less complex architecture (1.2), non-requirement of extra devices and its dependency on the PA linearizer setup only. It is used for amplifier characterization and tracking its behavior. Its application involves estimating the distortion characteristic of RF PA and then creation of its precisely complementary distortion characteristic and cascading the two in order to ensure that the resulting system has negligible input-output distortion. The cascade of the complementary distortion element after the RF PA is referred to as *postdistortion* (Figure 1.2).

However, post-distortion will require cancellation at high power and additional high power amplifier to amplify the distortion at the output of PA. Therefore, most of the complementary distortion systems are based around predistorting the input signal before sending it to PA, which is referred to as PD techniques.

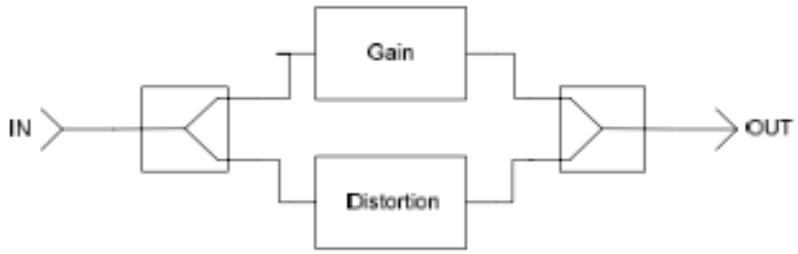

Figure 1.2 Post-Distortion Technique

PD techniques can be classified into analog, digital or hybrid, depending upon the type of application and the order of nonlinearity in the system, as shown in Figure 1.3.

Analog PD linearizers shown in Figure 1.3 (a) are small and inexpensive and can work at RF frequencies. However, analog predistorters typically fall short of the accuracy required for correcting all of the terms involved. Hence, they have generally been used to focus on the third-order inter-modulation components for low Peak-Average-to-Power Ratio (PAPR) signals [22]. The automatic control circuitry is often needed to ensure tracking over all corners of the operational specification [23]. Moreover, to compensate for higher-order IMDs in multicarrier systems, more complex circuits may be required [24]. Digital baseband predistortion (DPD) methods, as shown in Figure 1.3 (b), have been popular in recent years, due to their accuracy and less complexity in signal processing.

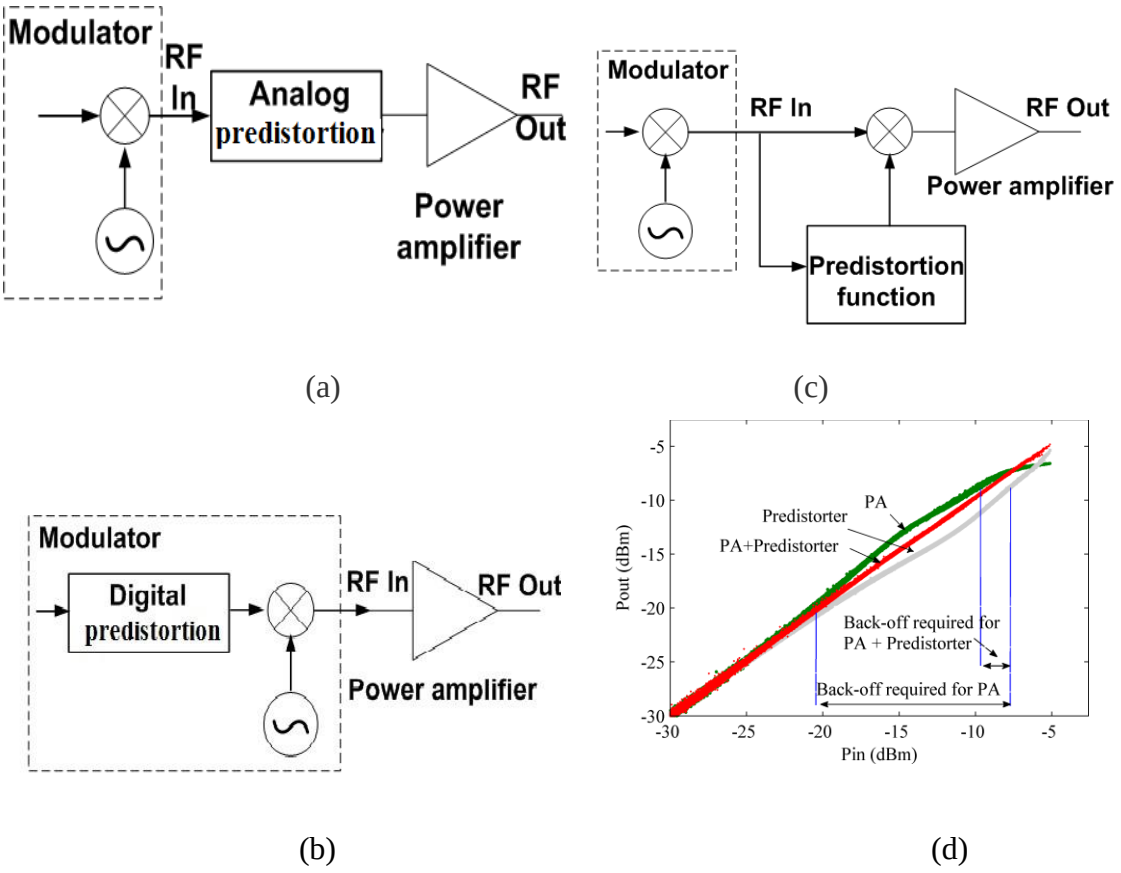

Figure 1.3 Predistortion Scheme. (a) Analog predistortion (b) Digital predistortion (c) Hybrid RF-digital -predistortion, (d) Predistortion operation.

The DPD technique depend on a digital baseband input and thus holds disadvantages in terms of system architecture, and the computational speed of the digital circuits limits the operational bandwidth. The power consumption of a digital signal (DSP) processor is directly related to operating frequency and the higher computational speed leads to higher power consumption [25]. The hybrid RF/digital predistortion (RF-DPD) is a compromise between analog RF PD and digital baseband DPD [25]-[28].

A simple block diagram is shown in Figure 1.3 (c). As compared to analog approaches, this PD architecture uses an adaptive DSP technique that achieves more accurate linearization. In addition, this architecture has advantages over conventional digital baseband approaches in that instantaneous correction occurs through the use of RF circuits without being limited by DSP speed and a 20-33 % wider correction bandwidth is achievable for third- to fifth-order distortions at the same clock speeds. Since it is nonparametric and does not rely on any knowledge of the signal structure, linearization can be performed without the need for exact digital baseband input signal. Therefore, the hybrid RF-DPD techniques are also suitable for repeater systems.

Figure 1.3 (d) shows the non-linear characteristics of PA and DPD in terms of output power variation with respect to input power drive. From this figure, it can be observed that the inverse non-linear characteristic of DPD compensates for the PA non-linear behavior and cascade of the two results in linear operation. These non-linear characteristics can also be expressed in terms of non-linear gain and phase variation with respect to input power drive. The gain compression characteristic is known as amplitude modulation to amplitude modulation (AM-AM) conversion, which is shown in Figure 1.4 for a class AB PA. Similarly, the phase compression characteristic is known as amplitude modulation to phase modulation (AM-PM) conversion which is shown in Figure 1.5 for a class AB PA.

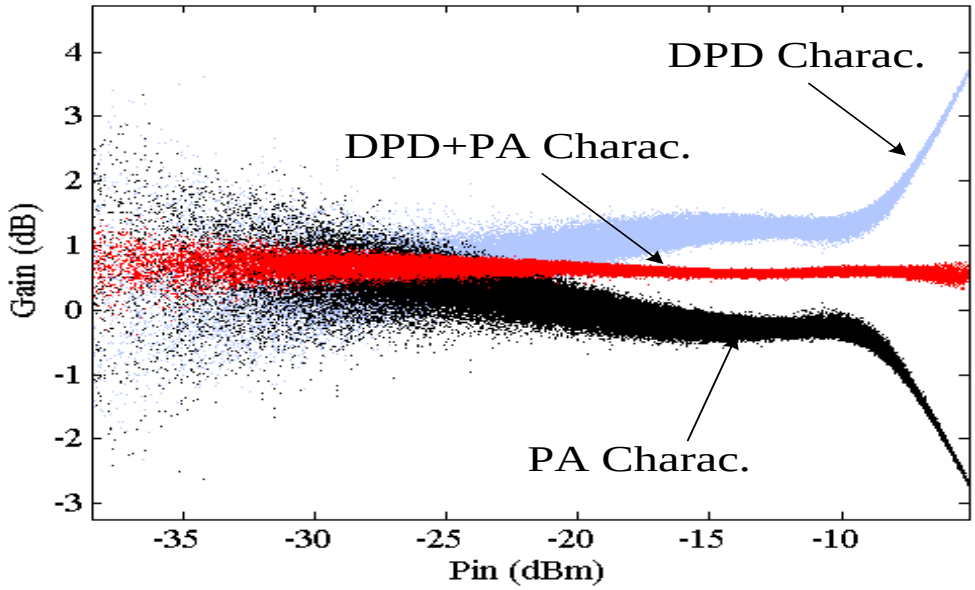

Figure 1.4 Non-linear phase compression characteristic (AM-AM) and its correction.

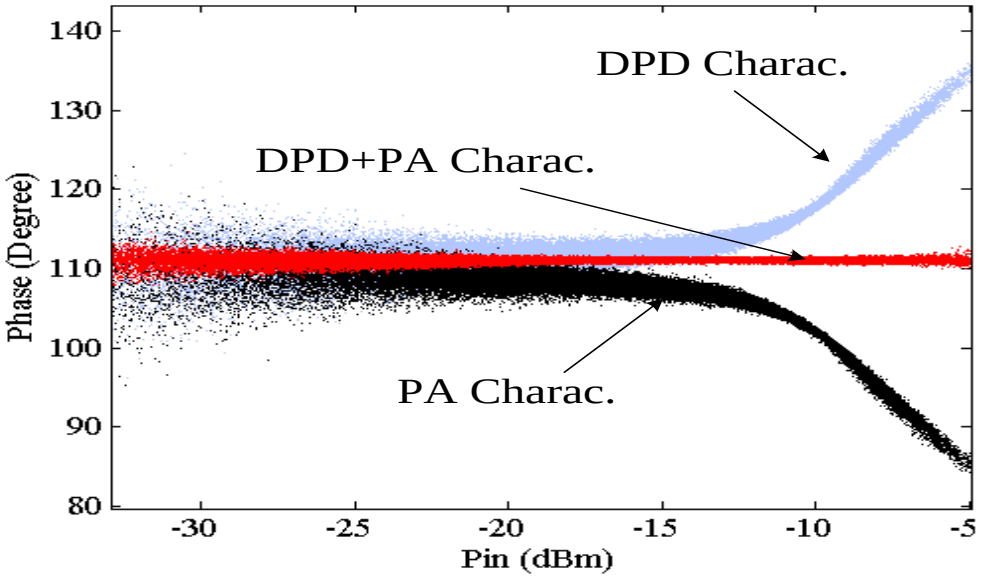

Figure 1.5 Non-linear phase compression characteristic (AM-PM) and its correction.

1.4 Problem Definition and Targeted Goals

The currently used DPD technique requires implementation of a suitable nonlinear function for getting best possible behavioral modelling [9] for better in-band [10] and out-of-band [10] modeling performance while using 3G+ signals. Memory polynomial is most popular and simple solution for DPD. However, when nonlinearity order of PA is high, due to increasing observation matrix size, model solution becomes less stable and more perceptible to input signal variations. Therefore there is a need to investigate new architectures for more accurate solution as well as more stable solutions.

Moreover, MP function [9-10] and its variations require access to digital domain complex data, however in many practical situations; the PA providers have access to only RF domain data. Keeping this requirement in mind, a suitable variation of memory polynomial, namely envelope memory polynomial has been investigated which requires access to only envelope or absolute value of input signal for its functioning as hybrid PD. The goal targeted here is the investigation of suitable models, which can provide good modeling performance, numerically stable solution and applicable when only RF signal is available.

1.5 Statement of Objectives

Based on the proposed architecture, the specific objectives of the proposed research were set in the beginning phase of the research. For the proof of concept, implementation of different polynomial function has been done and their performances has been studied with the aim to get the best possible modeling performance in terms of its in-band and out-of-band characteristics and stability of solution. The corresponding research objectives are listed as below.

Objective 1: Study and analysis of different polynomial functions with respect to MP function and that can be used for DPD implementation. Also, the operation and study of the polynomial functions with different non-linearity order and memory depth is performed.

Objective 2: Identification and analysis of the most suitable polynomial function and search for the modes in which it can be used for best results. The analysis includes implementation of original as well as modified form of polynomial functions like Zernike Memory Polynomial (ZMP) model and Pseudo-Zernike Memory Polynomial (PZMP) model, which can be best suited for the requirements.

Objective 3: Identification of numerically stable models for PA and inverse PA modelling.

Objective 4: Assessment of proposed model for PA using different 3G+ signals.

Objective 5: Study and implementation of hybrid RF-DPD scheme for RF-in and RF-out system.

1.6 Thesis Outline

According to the objectives defined for the proposed research, the entire thesis is divided into five chapters.

The first chapter focuses on describing goal and proposed methodology adopted over the existing state of art in order to full-full the defined objective of the thesis.

The second chapter involves the analysis PZMP model for different 3G+ signals and compares its performance in terms of its in-band [10] and out-of-band [10] characteristics for behavioral modeling. This work has been accepted to be published in the journal with following details:

P. Rawat, M. Rawat, N. Boulejfen and F.M. Ghannouchi, "Pseudo-Zernike polynomials for numerically stable PA modeling using 3G+ signals" Microwave and Optical Technology Letters, Article ID: MOP28642.

The third chapter involves the design methodology and consideration for two-step rational polynomial (RP) function [32] for accurate modeling of non-linear PA. For further study, its comparison with MP model is performed. This work is to be submitted in IEEE Transaction on Broadcasting.

The fourth chapter focuses on the study of FPGA based hybrid RF-DPD system for linearization of PA. The strategy of compensating IQ impairments in such system has been proposed for static linearization scheme. The study of the behavior of 3G+ signals with FPGA. The system has been theoretically applied for DPD using FPGA and the problem faced during DPD application on same in discussed.

The fifth chapter summarizes the contribution of the thesis and lists possible future extension of the current work for digital predistortion of single and multi-band application.

Chapter Two: Pseudo-Zernike Polynomials for Numerically Stable PA Modeling Using 3G+ Signals

2.1 Introduction

A power amplifier, being a vital nonlinear component of transmission system, has had a lot of interest in its black-box modeling for use in system level analysis of communication systems [34]. Although many parametric models have been proposed over time [9]-[35], memory polynomial is still considered the most simple and effective parametric model [36].

One of the main concerns while using the memory polynomial based modeling is the numerical instability of polynomial solutions, which in turn depends on conditioning of observation matrix created during modeling process. When matrix conditioning is high, small change in input characteristics may lead to large deviation from optimum result. As a solution to this, in [37] orthogonal memory polynomial (OMP) is proposed. These orthogonal polynomials are derived under the assumption that input signals have uniform probability density (PDF), However, PDFs of commercial signals such as WCDMA and WiMAX are far from uniform. It leads to deterioration in matrix conditioning of OMP.

In literature, odd or even order Zernike polynomials are known to form an orthogonal polynomial set, allowing for a better conditioned observation matrix. Utilizing this property, Zernike memory polynomials (ZMP) are proposed for either even or odd ordered polynomial models [38]. However, for proper modeling of power amplifier all terms (even and odd), have significance while using broadband modulated signals such as WCDMA, WiMAX etc. [36]

This chapter presents PZMP model, which is independent to input signal PDF and contains all terms (even and odd). It is shown in the following sections that PZMP provides more robust

performance with respect to previously proposed orthogonal models when input signal PDF is deviated from uniform distribution.

2.2 Pseudo-Zernike Memory Polynomial Model

Bhatia proposed PZMP in [39] mode in search of a complete orthogonal basis function's set, invariant to the phase rotation around the origin, which is given as follows:

$$U_n^{\pm m}(r,\theta) = R_n^{\pm m}(r)e^{\pm im\theta} \tag{2.1}$$

where, *n* and *m* are integers, such that $0 \le |m| \le n$ and $R_n^m(r)$ are radial polynomials given by:

$$R_n^{\pm m}(r) = \frac{r^{-(m+1)}}{n-|m|!}\left\{\left(\frac{\partial}{\partial(r)}\right)^{n-m}\left[(r)^{n+m+1}(r-1)^{n-m}\right]\right\} \tag{2.2}$$

where *r* lies within a unit circle ($r \in (0,1)$). The explicit formula for a circular Zernike polynomial is derived in [39]. From eq. (4.5) of [39], the expression of PZPM can be written as,

$$R_n^{\pm m}(r) = \sum_{s=0}^{n-m} \frac{(-1)^s.(2n+1-s)!}{s!(n-m-s)!(n+m+1-s)!} r^{n-s} \tag{2.3}$$

then resultant PZMP model is given by:

$$U_n^{\pm m}(r,\theta) = \sum_{s=0}^{n-m} \frac{(-1)^s.(2n+1-s)!}{s!(n-m-s)!(n+m+1-s)!} r^{n-s} e^{\pm im\theta} \tag{2.4}$$

By selecting *m*=1 and inverting the order of polynomial by substituting *l by n-s*, we can derive the following simplified expression:

$$U_n^{\pm m}(r,\theta) = \sum_{s=1}^{n} \frac{(-1)^s.(l+n+1)!}{(n-l)!(l-1)!(l+2)!} r^s e^{i\theta} \tag{2.5}$$

Now we compare (2.5) with the memoryless polynomial model in polar form given as follows:

$$y_{MP}(n) = \sum_{k=1}^{K} a_k e^{jf(n)} |r(n)|^k \tag{2.6}$$

where, ϕ and *r* respectively are phase and amplitude of input signal at instant *n*. If we compare (2.6) and (2.5), it can be readily observed that polynomial presented by (2.5) contains all terms of baseband polynomial model shown in (2.6). However each term is multiplied by an extra constant term decided by *l* and *n*. The only difference is that the (2.5) also contains and extra variable *l*. Therefore, similar to 'orthogonal memory polynomial' we introduce an upper triangular matrix given by:

$$U_{lk} = \begin{cases} (-1)^{k-l} \dfrac{(k+1+l)!}{(k-l)!((l-1)!(l+2)!)} & \text{for } l \le k \\ 0 & \text{for } l > k \end{cases} \tag{2.7}$$

This upper triangular matrix is dependent on *l and k* and according to (2.5), when it is multiplied with corresponding polynomial orders, they create an orthogonal set.

For introducing memory effect, the same upper triangular matrix will be multiplied with the polynomial set of each delayed data. Therefore, by introducing memory effects, the resultant PZMP model can be given by

$$\tilde{y}_{PZP}(n) = \sum_{k=1}^{K} \sum_{q=0}^{Q} \Lambda_{k,q} \psi_k(r(n-q)e^{if(n-q)}) \tag{2.8}$$

where $\Lambda_{k,q}$ are the model coefficients, and ψ_k are the basis functions given by:

$$\psi_k(x) = \sum_{l=1}^{k} U_{lk} e^{i\phi(n)} r(n)^l \tag{2.9}$$

where ψ is an upper triangular matrix . In the rectangular form, above equations can be summarized as follows:

$$\tilde{y}_{PZP}(n) = \sum_{k=l}^{K} \sum_{k=1}^{l} \sum_{q=0}^{M} \Lambda_{k,q} U_{lk} x(n-m).|x(n-m)|^k \, abs(x) \tag{2.10}$$

For such a model, the coefficient's vector, represented by Λ, can be easily estimated using the Least Square (LS) method as follows:

$$\Lambda = (\xi^H \xi)^{-1} \xi^H Y \tag{2.11}$$

where $(.)^H$ denotes the Hermitian transpose, and ξ represents the observation matrix and due to presence of Y matrix, this coefficient have an index function of memory.

It can be observed that (2.7) seems to have similarity in presentation to OMP [37] model, however next section will show that performance of proposed PZMP model is more robust as compared to OMP model when different signals are used.

2.3 Pseudo-Zernike Polynomial Model Performance in the presence of Non-Uniform Signal Pdfs

The robustness of proposed model is verified for input signals having two non-uniform PDFs namely (2.11) Rayleigh distribution and (2.12) Chi-square Distribution. Figure 2.1 shows the distribution of data for Chi-square and Rayleigh distribution signals. The figures have been plotted using 'hist' command in MATLAB, which shows histogram of data. In statistics, a histogram is a graphical representation of the distribution of data. It is an estimate of the probability distribution of a continuous variable. This is verified for input signals having two non-uniform PDFs namely (2.11) Rayleigh distribution and (2.12) Chi-square Distribution. Figure 2.1 shows the distribution of data for Chi-square and Rayleigh distribution signals. The figures have been plotted using 'hist' command in MATLAB, which shows histogram of data. In statistics, a histogram is a graphical representation of the distribution of data. It is an estimate of the probability distribution of a continuous variable.

From Figure 2.1, it can be observed that Rayleigh distribution represents mild non-uniform distribution while Chi-square distribution represents highly non-uniform distribution as compared to the ideal uniform distribution. This non-uniformity motivates the implementation of new

polynomial function models (PZMP) to cover up the drawbacks of previously proposed models (like MP and OMP).

The Rayleigh distribution is characterized by:

$$p(x) = \frac{x}{d} e^{-\frac{x^2}{2d^2}} \qquad \tilde{x} \; 3 \; 0 \tag{2.11}$$

where, x is input signal amplitude. The parameter δ is chosen to be 1. The Chi-square distribution is characterized by:

$$p(x) = \frac{1}{2^{k/2} \mathrm{G}\left(k/2\right)} x^{k/2-1} e^{-\frac{x}{2}} \qquad \text{for } 0 < \tilde{x} < ¥ \tag{2.12}$$

where k is the degree of freedom, which is chosen to be 5 randomly for observing non-uniformity in the input signal at any random instant, for the PDF shown in Figure 2.1.

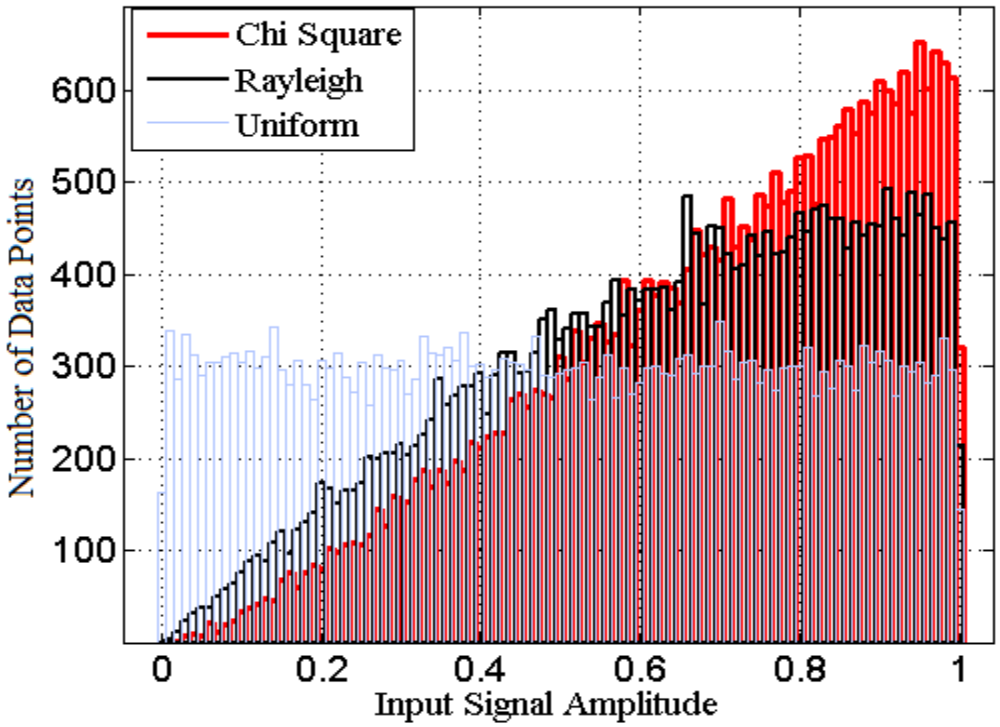

Figure 2.1 Histograms of Input signals having different distribution functions.

2.3.1 Observation Matrix Performance

The higher conditioning number is indicator of a badly conditioned observation matrix which makes the pseudo-inverse calculation very sensitive to slight disturbances. It may also lead to inaccurate results when finite precision calculation is used. On the other hand, a lower value of condition number indicates that the matrix is well conditioned, which means that there is less window for errors in the pseudo-inverse calculation and more stability against slight or mild disturbances. As we are using LS method which is based on norm-2 error cost function, we used norm-2 condition number, κ , given by:

$$k(\psi) = \|\psi\|_2 \|\psi^{-1}\|_2 = \frac{\sigma_{1,A}}{\sigma_{2,A}} \tag{2.13}$$

where ψ is matrix to be inverted. $\sigma_{1,A}$ and $\sigma_{2,A}$ are smallest and highest eigen values calculated for Vandermonde matrix using single vector decomposition [10]. As shown in Figure 2.2, the PZMP model gives more than 50% improvement in terms of condition number (in dB) as compared to OMP Model for both Chi-Square (2.11) and Rayleigh (2.12) distribution because of independency of PZMP model on PDF of the input signal. Clearly, when input signal PDF is not uniform, PZMP model have more robust performance as compared to OMP model as shown in Figure 2.2.

Proposed model's parameters are obtained using equation 2.11. It is to be noted from (2.7) that **U** is a matrix, which is not dependent on input signal, therefore all elements of **U** are constants independent of *x*(*n*). Eventually **A** in MP model is equivalent to $\mathbf{\Lambda U}$ in PZMP model and original MP relation between input data and output data is maintained. The detailed mathematical proof to

show that multiplication of MP model with triangular matrix retains simplified Volterra relation can be found in [37].

Therefore, if MP model calculates coefficients a's (2.6) in the relation (**Y=AX**), PZMP model calculates coefficients **Λ** 's in the relation (**Y= Λ UX**) where U is a constant upper triangular matrix already known from (2.7).

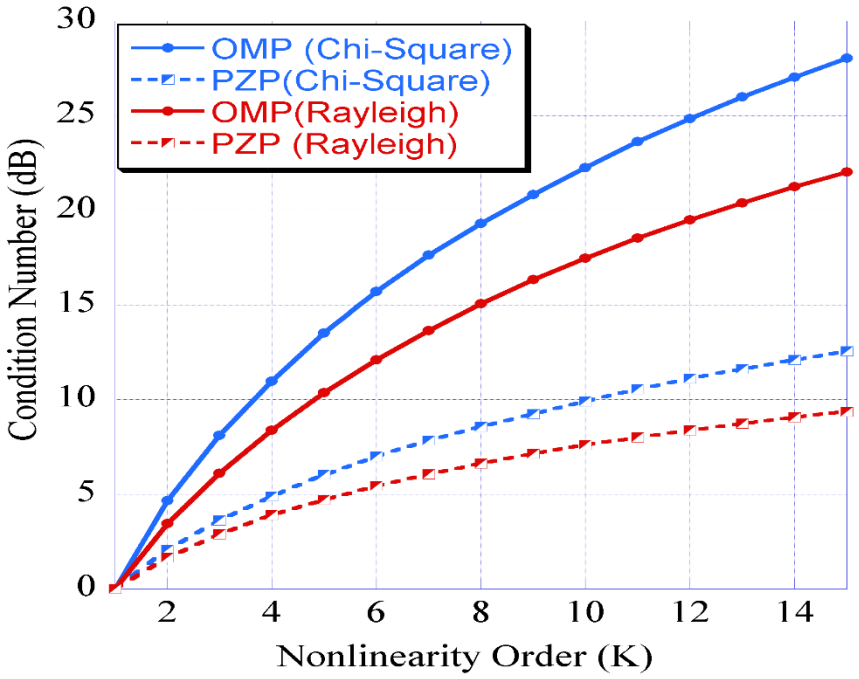

Figure 2.2 Condition Number (in dB) of observation matrix for OMP as well as PZMP for memory less case

2.4 Model Performance of Different Polynomial Models for 3G+ Signals

The above study (in section 2.3 and Figure 2.2) simply shows that orthogonal polynomial performances in terms of condition numbers are tied to the signals with different PDFs. Thus, in

this section we study the model stability performances of different polynomial models. Figure.2.3 shows the PDF of the practically used 3G+ signals used for the modelling.

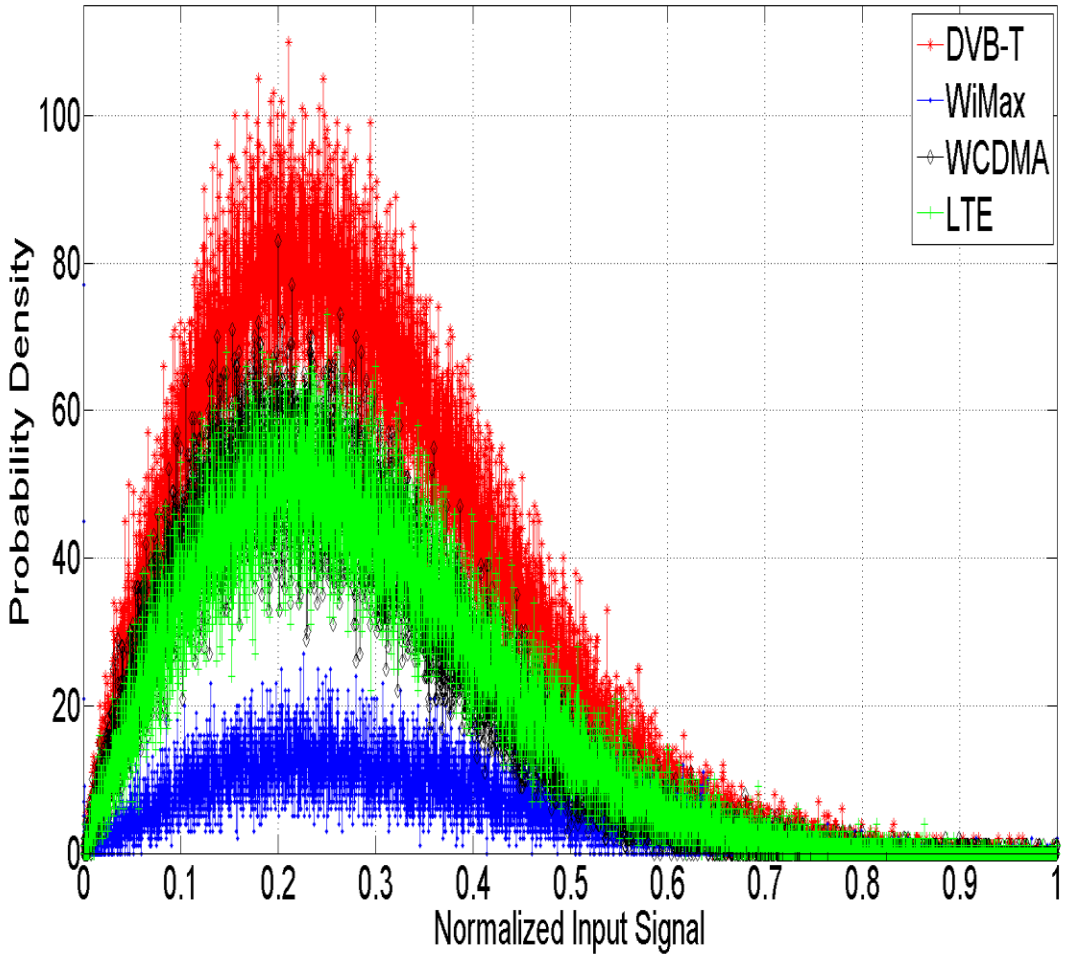

Figure 2.3 Probability density functions of different signals

Table 2.1 Condition No. (in dB) for 3G+ Signals

SIGNALS		MPM (dB)	OMPM (dB)	PZMP (dB)
Class AB	**WCDMA 101**	177	60	78
	Wi-Max	196	85	75
	DVB-T	157	84	74
	LTE	163	90	98

Table 2.1 shows the effect of three different models, MP, OMP and PZMP models, respectively, on the condition number of the WCDMA [5], WiMAX [6], DVB [7] and LTE [8] signals.

From model implementation point of view, dispersion of model coefficients is also considered an important criterion [10], which is given as follows:

$$c(A) == \frac{\max(|a_{ij}|)}{\min(|a_{ij}|)} \tag{2.14}$$

where $\max(|a_{ij}|)$ and $\min(|a_{ij}|)$ represents maximum and minimum value of the coefficients of the observation matrix A. Dispersion coefficient is used in digital predistortion based literature to see the dispersion of model coefficients. If dispersion coefficient is high, this means that the coefficients are dispersed in a large dynamic range and requires the use of precise processor. When

using an embedded processor, running fixed-point calculation, this will lead to low resolution and inaccurate results.

Table 2.2 indicates the effect of three different models, MPM, OMPM, and PZMP on the model dispersion coefficient while using four different 3G+ signals, that are, WCDMA [5], WiMax [6], DVB [7] and LTE [8] signals, used in the measurement.

Table 2.2 Dispersion Coefficients (in dB) for 3G+ Signals

SIGNALS		**MPM**	**OMPM**	**PZMP**
Class AB	WCDMA-101	64	38	19
	WiMax	65	40	18
	DVB	47	42	28
	LTE	38	30	21

It is noticed that with the proposed model, a considerable reduction in the condition number is observed for DVB and WiMAX signals, while the dispersion number is improved significantly as compared to traditional orthogonal polynomial model for all the signals. Condition and dispersion numbers have two scenarios of direct impact on application of PA modeling because,

1. In the implementation of model in FPGA for DPD application, the FPGA consumes significantly less resources for fixed-point calculation as compared to floating point calculations. It is established that when model observation matrices are better conditioned

[11], they provide much better performances in fixed-point calculation scenario. Low condition number ensures better conditioning.

2. When power amplifier is very nonlinear, polynomial with high nonlinearity order is required. In such case, due to bulky observation matrix, matrix conditioning has direct impact on the precision of the pseudo-inverse calculation and therefore on the model performance. A well-conditioned matrix will have its inverse calculated with good accuracy. As a result, the predistortion model is more accurate than in the case of an ill-conditioned matrix.
3. The number of bits used to represent the model coefficients and the type of arithmetic – floating point versus fixed point – used in the coefficient extraction and the application of the predistortion functions, has direct relation to power consumed by DSP. Therefore, a low value of the dispersion coefficient ensures that fixed point computation and low number of bits can be used, which leads to less complexity and less DSP power consumption and thus better cost efficiency.

Fig. 2.4 shows adjacent channel error power ratio (ACEPR) for out-of-band performances for PZMP, OMP and MP models [10], which is given by

$$ACEPR_{dB} = 10\log_{10}\left(\frac{\int_{\omega 1}^{\omega 2}|E(f)|^2\,df}{\int_{\omega 3}^{\omega 4}|Y_{in}(f)|^2\,df}\right) \tag{2.15}$$

where $Y_{in}(f)$ represents the power of the input signals within the band $\omega 3$ and $\omega 4$ $E(f)$ the error power of the adjacent channels $\omega 1$ and $\omega 2$.

Fig. 2.5 shows normalized mean square error (NMSE) for in-band performance [10], which is given by.

$$NMSE_{dB} = 10\log_{10}\left(\frac{\int_0^N |E(k)|^2\, dk}{\int_0^N |Y_{meas.}(k)|^2\, dk}\right) \tag{2.16}$$

where N represents the number of data samples, E represents the error in the measured signal and Y represents the measured signal.

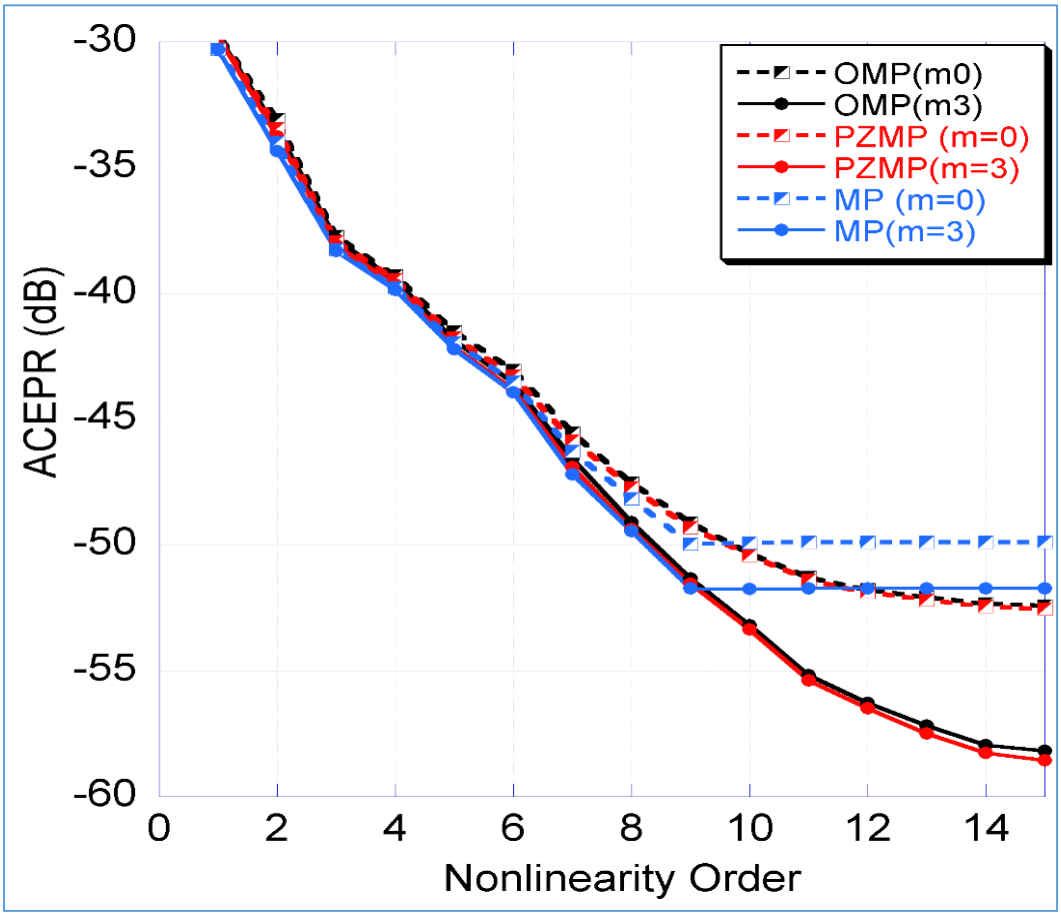

Figure 2.4 Comparison of ACEPR Performances

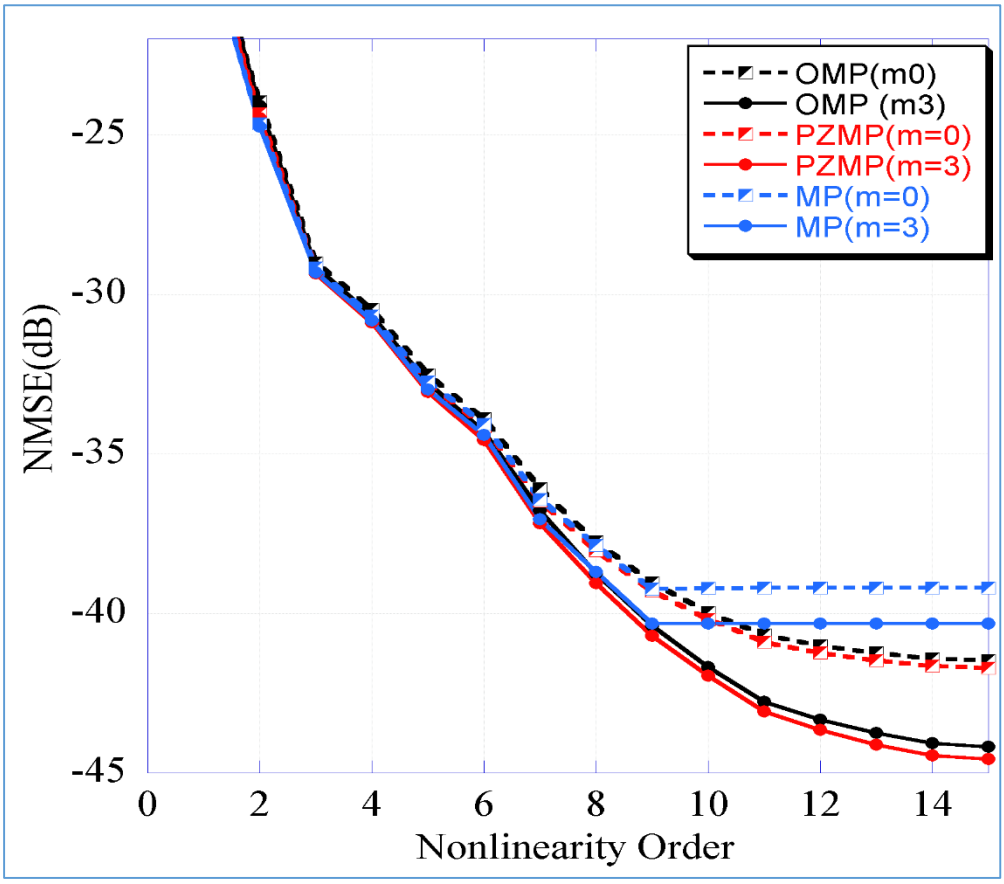

Figure 2.5 Comparison of NMSE Performances

It is evident that even when both models are representing the same simplified Volterra function [10] to model PA output, NMSE and ACEPR performances are significantly improved for OMP and PZMP model at higher orders due to better-conditioned matrices. Moreover, PZMP model have slightly better in-band and out-of-band performances in memoryless, as well as, optimum memory depth scenario.

The MP model saturates after non-linearity order 10 (as shown in Figure 2.5) because after a certain high non-linearity order, the numerical instability approaches in saturation for this reason, we observe no considerable change in MP model performance in terms of in-band and out-of-band

performances. The PZMP model instead of being independent of non-uniformity of input signals is giving slightly better performance than the OMP Model. This is because practically PDF of input signal affects the performance of PZMP model and thus a little deterioration in the model performance is observed.

In essence, with similar kernel terms for OMP and PZMP, PZMP could replace OMP models with similar complexity and improved performances for practical 3G+ signals.

2.5 Conclusion

This chapter investigated a Pseudo-Zernike memory polynomial model [31], which provides an alternative to replace OMP, and MP models for more stable numerical solutions and less dispersed model coefficients, when input signals have non-uniform PDFs. The performance of Pseudo-Zernike based model is compared with orthogonal polynomial based model for practically used signals and it has been observed that the proposed model provides polynomial model with significantly less dispersed coefficients.

Chapter Three: Rational Function Based Two-Step Model for Accurate Modeling and DPD for High Power Amplifiers

3.1 Introduction

Due to increasing need of wireless data communication systems from technical and social perspective, there is a strong motivation towards research related to PA designs for transmitters and receivers. New designs of such devices and circuits require access to system level behavior modeling techniques. Behavioral modeling is a simple and popular method to create digital models to be used in a simulation and to emulate complex systems driven by highly time varying signals Figure 3.1 shows output for a nonlinear transmitter [34], where adjacent band distortion is generated in the system because of the PA nonlinearity.

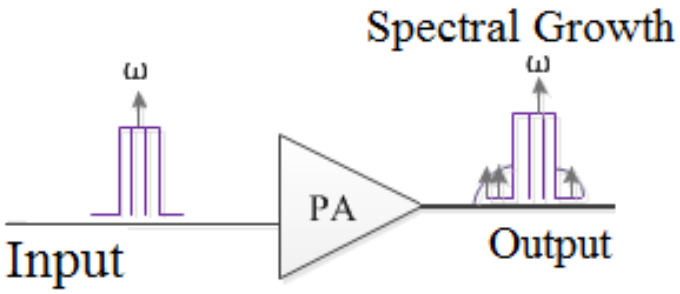

Figure 3.1 Signal distortion and resultant spectrum re-growth due to PA Non-linearity.

State-of-the-art behavioral modeling approaches have mostly been reported using polynomials and splines [34]. These polynomial based models are further improved by including memory-effects

[40]-[41] in the form of time-delayed input signals. It has been reported in literature ([36] and references therein) that a physical analogy of PA is a feedback system, therefore recursive models, including feedback from output, might provide a more physical representation of the PA and, thus, provide more accurate modeling performance [10]-[32]. In view of these theoretical considerations, recursive models such as recurrent neural network and rational functions have been proposed for the behavioral modeling of a single band transmitter [33]-[42]. However, in such recurrent models, due to close loop system, there is always an issue of system stability. Therefore, this chapter proposes a novel two-step rational polynomial function based behavioral modeling approach for the single band transmitters, which provides more promising modeling performance near band of interest as compared to the common approach using single step input-output data from measurement setup.

3.2 State-of-the-art memory polynomial model

Considering *x* and *y*, the input and output baseband signals at the given carrier frequencies, the generalized complex baseband input/output relationship of the memory polynomial model for the single band transmitter, with *k*th nonlinearity order, is expressed as [34],

$$y(n) = \sum_{k=0}^{K} \sum_{m=0}^{M} c_{p,m}.x(n-m).\left|x(n-m)\right|^{k} \tag{3.1}$$

where $c_{p,m}$ is the coefficient of the model and M represents the memory depth. The MP model is one of the reliable and primitive polynomial method.

3.3 Rational function model

The rational polynomial method proposed here, works in robust performance mode [36] and is used for the behavioral modeling as follows

$$y(n) = \frac{f_N}{1 + f_D} \tag{3.2}$$

where, f_N and f_D are numerator and denominator non-linear terms given by:

$$f_N = \sum_{i=0}^{K_n} \sum_{m_n=0}^{Mn} a_{i,m_n}.x(n - m_n).\left|x(n - m_m)\right|^{i-1} \tag{3.3}$$

$$f_D = \sum_{j=0}^{K_d} \sum_{m_d=0}^{Md} b_{j,m_d}.x(n - m_d).\left|x(n - m_d)\right|^{j-1} \tag{3.4}$$

where K_n and K_d are the nonlinearity orders for the numerator and denominator of the given function respectively; and M_n and M_d represents the memory depths used in the numerator and denominator, respectively. Equation (3.2) represents the ratio of two MP models [41]. RF can also be written in the following recursive form:

$$y_R(n) = f_N - y_R(n).f_D \tag{3.5}$$

From (3.5), it can be observed that, in terms of coefficients, the proposed model is linear for representing N samples of the input signal can be defined as:

$$\vec{y} = [y(n), ..., y(n+N)] \tag{3.6}$$

The observation matrix comprises of numerator and denominator terms, which are defined as follows:

$$\vec{g}(n) = [x(n).|x(n)|^{i-1}, ..., x(n-1)|x(n-1)|^{i-1}, ..., x(n-M_n)|x(n-M_n)|^{i-1}]^T \tag{3.7}$$

$$\vec{b_i}(n) = -y(n).[x(n).|x(n)|^{j-1}, ..., x(n-1)|x(n-1)|^{j-1}, ..., x(n-M_d)|x(n-M_d)|^{j-1}]^T \tag{3.8}$$

$$\vec{g} = [\vec{g}(n), ..., \vec{g}(n+N) \tag{3.9}$$

$$\vec{b_i} = [\vec{b_i}(n), ..., \vec{b_i}(n+N)] \tag{3.10}$$

$$G = [\overrightarrow{g_{0,0}}]...[\overrightarrow{g_{Nn,Nn}}][\overrightarrow{b_{0,0}}].....[\vec{b}_{Nd,Nd}] \tag{3.11}$$

If coefficient vector for rational model is given as follows:

$$\alpha = [a_{0,0}, ..., a_{Nn,Nn}, b_{0,0}, ..., b_{Nd,Nd}]^T \tag{3.12}$$

The rational model can be given as follows:

$$\vec{y} = \alpha \times G \tag{3.13}$$

The coefficients can be calculated using the LS solution. In this chapter LS has been implemented according to the singular value decomposition (SVD) method.

3.4 Two-step RF model description

The RF model for the modeling performances generally uses one step extraction and processing of the available polynomial function. As per author's best knowledge, less consideration is given to multi-step extraction of the polynomial function, which can enhance the modeling performance of the system.

In this chapter, two-step extraction of the given polynomial function is performed to allow for non-recursive topology. The coefficients are extracted using the stored values of input and first step extraction output denoted as $x(n)$ and $y(n)$ (3.8), to provide a robust model. The application of recursive can provide us with promising outcomes, but the output at the present time remains unknown beforehand for most of the practical applications of behavioral modeling. Therefore, to avoid this shortcoming, generally the model output is calculated in the form of rational function (3.2). The rational function output shows no significant improvement in terms of modeling performance as reported in [9], but is observed to be useful for reducing model complexity as calculated in (3.2). It is shown in Section 3.5 that performance is significantly degraded using the rational function form given in (3.2) as compared to its recursive form given in (3.5).

This chapter proposes the use of two-step coefficient extraction method for rational function models for better modeling performance, utilizing its recursive property. In first step, the conventional MP model [40] is extracted, followed by the use of modeled output of the MP model of the first step as one of the input to the RF in the second step. The signal processing flow-chart for the two-step RF model is shown in detail in Figure.3.2.

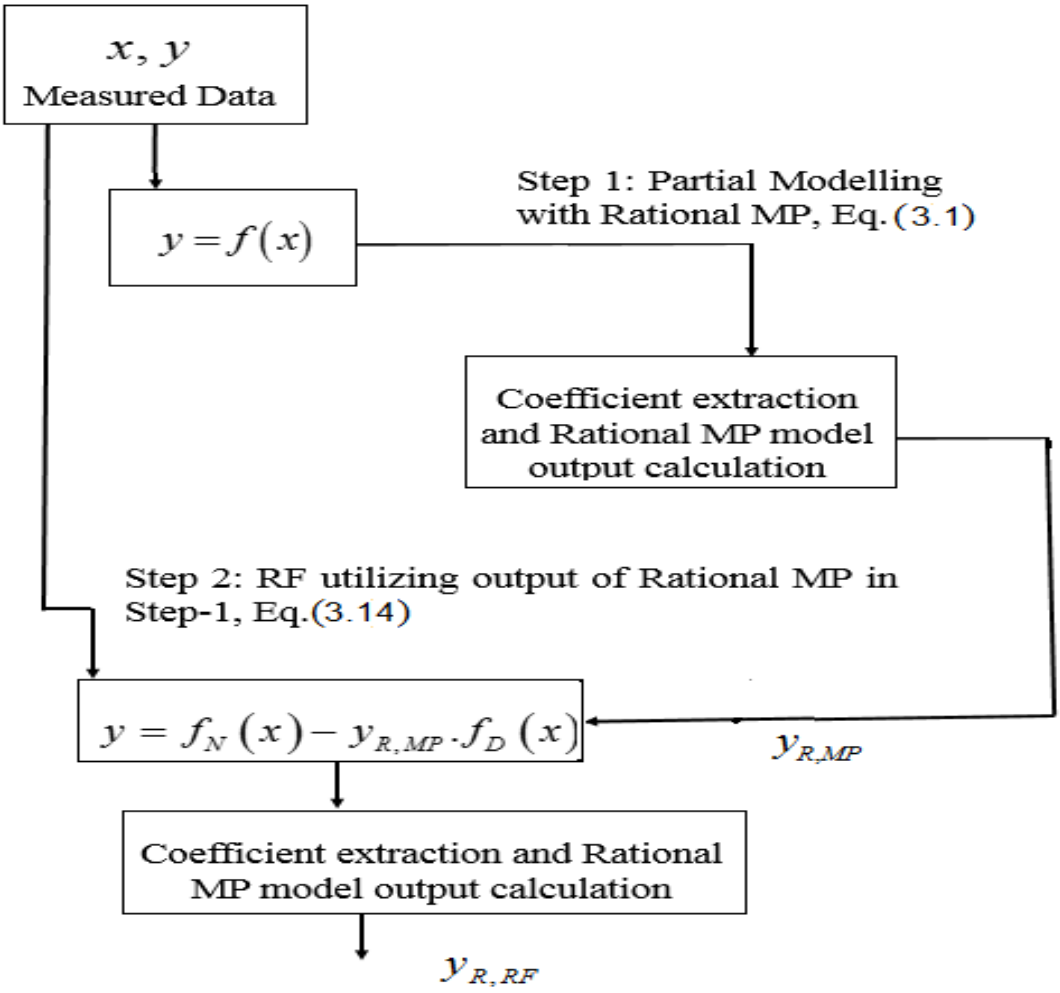

Figure 3.2 Block-wise description of two-step rational function model

In two step RF model, eq. (3.5) can be written as follows:

$$y_R(n) = f_N - y_{R,\,MP}(n).f_D \tag{3.14}$$

where $y_{R,\,MP}(n)$ is MP model output of the first step. In the two-RF model, the first step provides the crude estimation of PA output, while the second step focuses more upon the refining and

tuning of the coefficients to provide minimum possible error. This model seems like the two-box and three-box models as described in [10]-[48]. However, there is an inherent difference between two-step rational function model and two-box model. The final stage of the proposed two-step RF model is directly dependent on input data, as well as the output of previous stage because an error in previous step can be adjusted due to the presence of the input data in the final stage.

It is better than the final stage in two-box and three-box models which depends only upon the output of previous stage as an error in the previous stage has direct impact.

3.5 Measurement Setup

The measurement setup for two-step recursive RF DPD is used for the behavioral modeling of the single band measurement and is shown in Figure 3.3. The measurement setup consists of a vector signal generator (VSG), a linear driver amplifier, a Class AB PA and a Vector spectrum analyzer (VSA). A PC interface is used to control the instruments and to download and upload the signal data files as per the requirement of the user. The driver Amplifier and Class AB PA are connected to the power supply that works below its work down voltage to ensure correct measurement and avoid any damage to the PA and components of the PA setup. The input in form of *I* and *Q* data is first loaded in the Agilent E4438C VSG as illustrated in Figure 3.3. The VSG is used to generate wireless signals in form of $\underline{I}+jQ$ format, which can be used as an input signal for PA and can be predistorted to check for its performance.

The driver amplifier provides a gain from the output of the signal generator to the input of the PA of about 30 dB. To bring the RF signal to receiver input signal power range, 40 dB of attenuation is used at PA output. The peak output power level from the PA is limited by putting a restriction on the allowable output power from the VSG. The settings in the VSA (reference level and input

attenuation) are set in such a way as not to distort the measured signal in the receiver, even for the highest peak power level [5]. This means that it will result in a considerable degradation in noise performance when using power levels lower than the maximum allowable level.

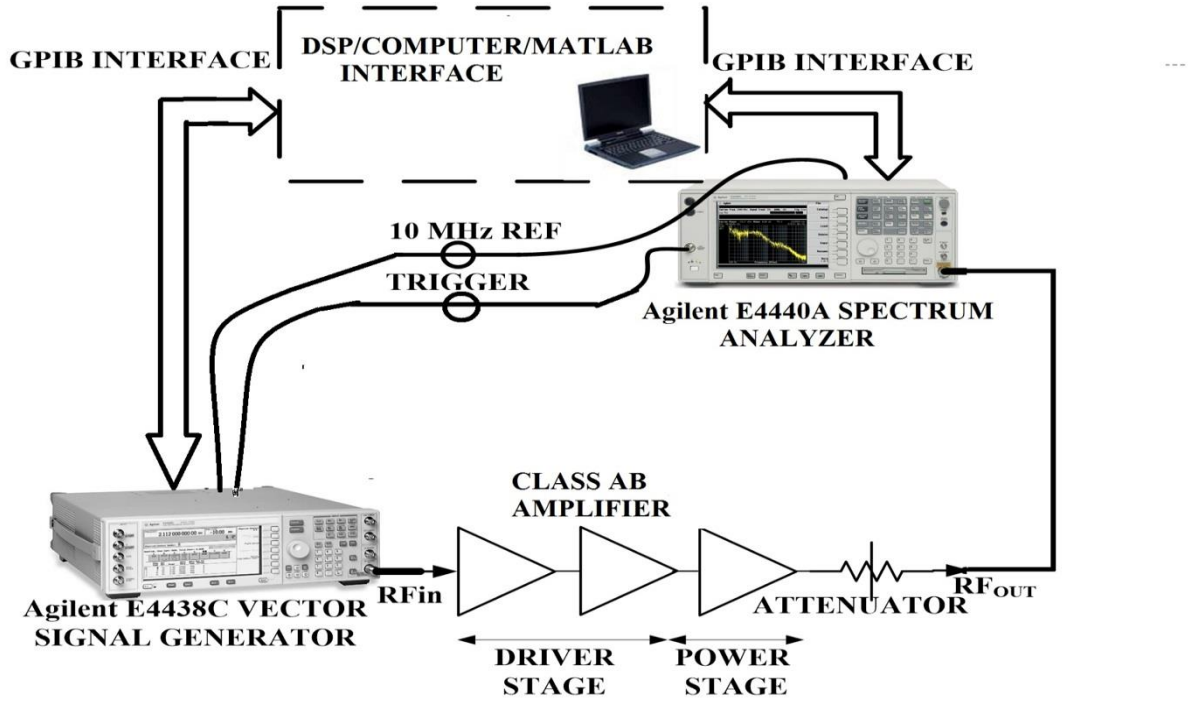

Figure 3.3 Measurement setup for the DPD using Class AB Power Amplifier

The measurement setup consists of:

- ✓ **Vector signal generator (VSG)**
- ✓ **Linear driver amplifier,**
- ✓ **Class AB PA ,1.96 GHz LDMOS**
- ✓ **Powerwave Doherty PA, 2.14 GHz LDMOS**
- ✓ **Vector spectrum analyzer (VSA).**

In the measurement setup, we first generate the base-band *I* and *Q* waveform signal using VSG. The baseband signal is modulated and up-converted using signal generator and pre-amplified by the driver amplifier in driver stage. The driver amplifier gain is approximately 30 dB. In power stage, the signal is amplified using Class AB PA. A 40 dB attenuator is used at PA output.

Class AB PA output is a distorted signal, depending upon the PA characteristics. The output from the PA is captured within the given band using a dedicated receiver. The stored data is time aligned for the give band using cross-correlation technique [60]-[61].

3.6 Modeling Performance

The proposed model is evaluated in terms of NMSE for the time domain modeling performance evaluation as described is previous chapter. The NMSE works better to deal with high power data and is considered a measure of in-band performance, while ACEPR provides a measure for the frequency domain and is used as a metric to assess the out-of-band modeling performance.

Table 3.1 shows the NMSE and ACEPR values achieved for two models, MP model (MPM) and 2-step-Rational Polynomial Model (RPM). The ACEPR results corroborate the improvement observed in Figure 3.4 and Figure 3.5.

For the NMSE results, RF model (Eq. 3.5) provides approximately 14-18 dB improvement over the MP model, while the proposed 2-step-Rational-RF model provides approximately 4-6 dB improvement over the RF model. Figure 3.4, Figure 3.5 and Figure 3.6 shows the model error power spectrum densities (EPSD) for the conventional MP model [40], the RF model and the two-step-Rational-RF models for different WCDMA signals.

Table 3.1 Comparison between MPM and RPM with different 3G+ signals for Class AB Amplifier

WCDMA SIGNALS	MPM		RPM	
	NMSE (dB)	ACEPR (dB)	NMSE (dB)	ACEPR (dB)
WCDMA_1	-41.35	-54.49	-42.50	-59.55
WCDMA_11	-43.71	-55.12	-45.99	-58.84
WCDMA_101	-41.12	-55.39	-44.65	-59.06
WCDMA_111	-41.67	-51.15	-44.75	-56.41
WCDMA_1001	-40.35	-54.25	-43.58	-58.35
WCDMA_1111	-38.55	-46.95	-41.90	-52.05

The conventional MP model achieved best performance with nonlinearity order = 8 and memory depth = 2 for the. The RF models achieved best performance with Kn = 8, Mn = 2, Kd = 0 and Md = 2.

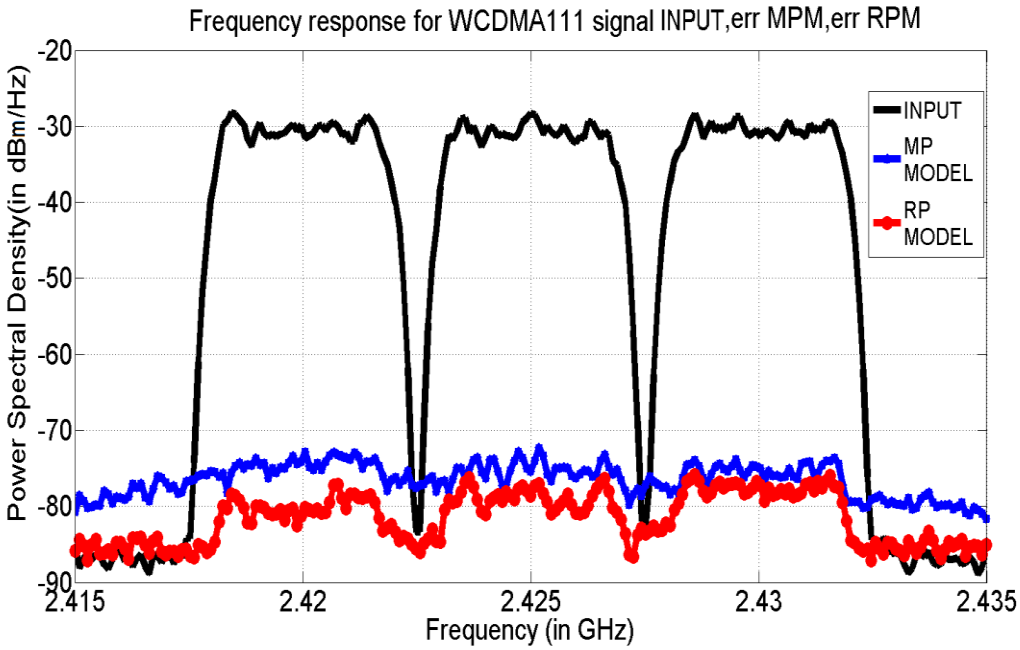

Figure 3.4 Spectrum of WCDMA_111 signal input (black), spectrum of the modeling error for MP (blue) and RP (red) Models

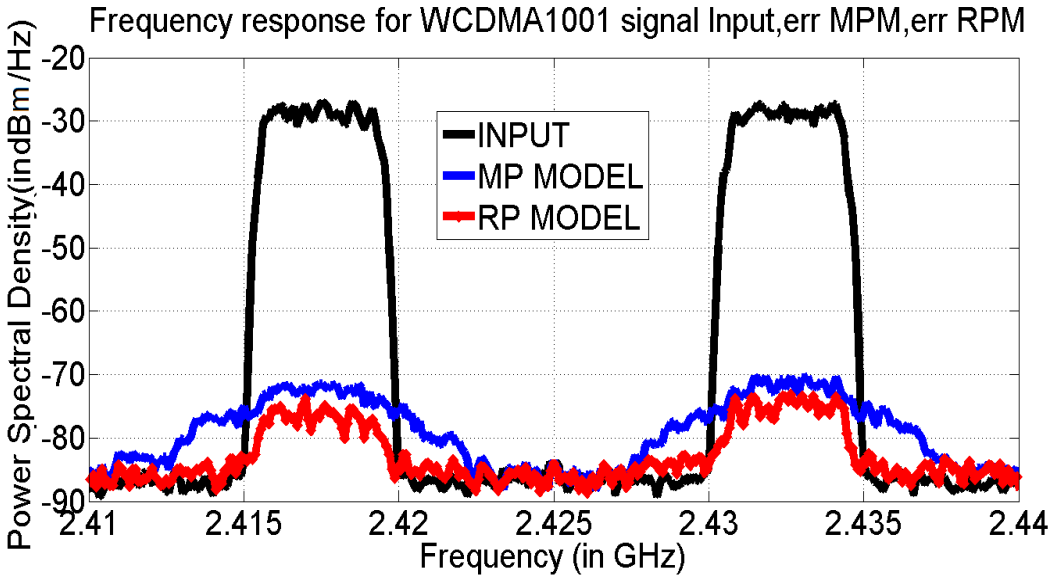

Figure 3.5 Spectrum of WCDMA_1001 signal input (black), spectrum of the modeling error for MP (blue) and RP (red) Models

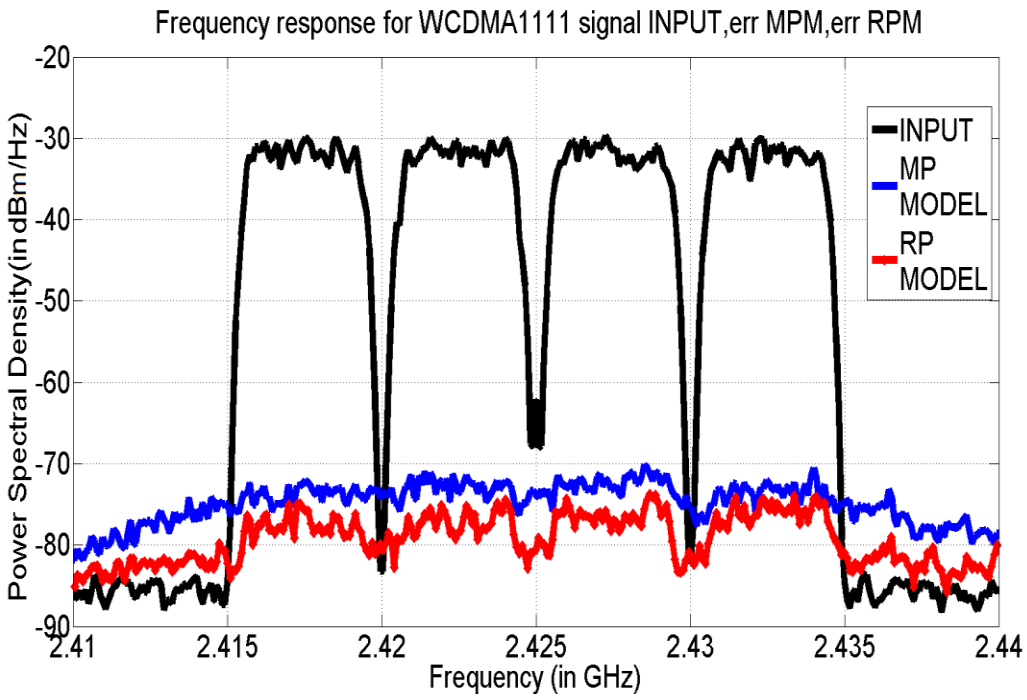

Figure 3.6 Spectrum of WCDMA_1111 signal input (black), spectrum of the modeling error for MP (blue) and RP (red) Models

For the Two-step-RF model, during first step, a memoryless MP model with nonlinearity order 4 is used, and the best performance is achieved for K_n=8, M_n=2,, K_d=8 and M_d =2 .

It is observed from Fig.3.4 that, with its recursive nature, the RF model (Eq. 3.5) improves EPSD by 12-15dBc on an average, as compared to the MP model.

However, its application cannot be widely used due to the limitation of its dependence on model output itself. The non-recursive RF Model form applied here is given by (3.2), provides poor performance as compared to conventional MP model. On the other hand, however, the proposed Two-step RP model exhibits 3-6 dBc improvements, on an average, in EPSD as compared to conventional MP model for complete frequency range.

3.7 Conclusion

This chapter proposes a rational function based behavioral modeling approach for accurate modeling and DPD of high power non-linear PAs. It has been shown with measurement data that the recursive property of rational function model [10], being closer to the physical analogy of PA as feedback system, allows for more accurate modeling. Based on the good performance of the two step RP function [10], a novel two-step model [48] has been proposed which retains advantages of recursive modeling, yet can be applied in an open loop configuration. This chapter proposes a model, which is compared with the MP model for behavioral modeling of high power amplifiers. Using the proposed model, performance improvement up to 3-dB in terms of NMSE and performance improvement up to 6-dB in terms of ACEPR is achieved, as compared to the MP model.

Chapter Four: Hybrid RF-Digital Predistortion System

4.1 Introduction

In RF PA linearization design, reducing the amplifier distortion is of the utmost importance. The PD [26]-[53] involves the creation of a distortion characteristic that is precisely opposite to the distortion characteristic of the RF PA, where the cascade of the two ensures that the resulting system has little or no input-output distortion. Since linearization is performed at the input of the PA, the loss of efficiency is negligible. A PD technique hybrid RF-DPD architecture has been proposed as a compromise between analog and digital PD techniques [13]-[55]. Hybrid RF-DFD has more accurate linearization, compared to analog PD architecture [52]; and the bandwidth is not limited by DSP computational speeds, since the signal correction (PD) is done directly on the RF signal under the control of the digital circuits [50], [26]-[55]. In addition, this architecture is nonparametric and does not require access to the digital baseband input signal. Therefore, the hybrid RF-DPD technique is suitable for stand-alone PAs and repeater systems [13].

The most common implementation issue in hybrid RF-DPD is the I-Q imperfections in the RF vector multiplier and associated circuitry [54]-[55]. The performance of hybrid RF-DPD is limited due to I-Q imperfections in these key components [13]. These imperfections cause errors, in terms of implemented gain and phase of the PD function. This chapter presents the methodology of implementing hybrid RF-DPD with LUT adapted to compensate for hardware related I-Q imperfections of the RF vector multiplier within the DSP domain. This modified LUT will accurately compensate for I-Q imperfection, without needing a precise tuning of the control voltages at the pins of the RF vector multiplier [13]-[26]. The test setup for characterizing the hybrid RF-DPD system is to obtain the I-Q imperfections which are also described and this

information is used to modify the LUT to compensate for these imperfections. To verify the capability of the modified LUT in compensating for the I-Q imperfections, linearizing a class AB base station PA operating at 1.960 GHz using the hybrid RF-DPD system, developed with an Altera Stratix FPGA evaluation board, carries out an experimental validation. EMP model is implemented on calibrated setup.

4.2 Background and design of Hybrid RF-PD System

The PA is a major component for successful working of transmitters, but at the same time, contributes to the nonlinearity in RF transmitters [49]. Due to its nonlinear characteristics, the PA exhibits AM-AM and AM-PM distortions. These distortions are prominent when the signal peaks approach the PA's saturation region, thus requiring some back-off of the average power level [49]. However, higher efficiency is obtained as the average power is increased. It is, therefore, desirable to extend the linear range of the PA as high as possible toward the saturation point, in order to obtain a reasonable trade-off between linearity and power efficiency [52].

Among various schemes for linearization like postdistortion and PD, the PD stands as the most promising, as it is more cost effective and least complicated one [54]-[18]. The DPD technique is one type of PD technique has been proposed for high non-linear orders as it is capable of numerically synthesizing PD functions with higher order nonlinearities, [51-55]. The reconfigurable feature of DPD and its functionality is digital domain, compatible with DSP units, makes it suitable for FPGA implementation. Contrary to Analog PD [53] which works over analog systems, the DPD technique has a wider scope and accuracy that makes it best suitable for base station amplifier linearization. However, this technique has two main disadvantages too, which prevents its sole acceptance in most of the applications.

1. The first con of DPD is its dependency to access the digital baseband complex signals driving the whole transmitter in digital domain, which makes it suitable for linearization of the whole transmitter, but not of the PA alone, in terms of system architecture.
2. Secondly, DPD has limited operational bandwidth as its implementation requires a relatively high speed of the digital and mixed circuits [55]. Considering the noticeable flaws in DPD implementation, a better technique is a hybrid DPD that is used here as it can compensate for the performance issue and provides better results. Figure 4.1 shows an overview of hybrid DPD technique.

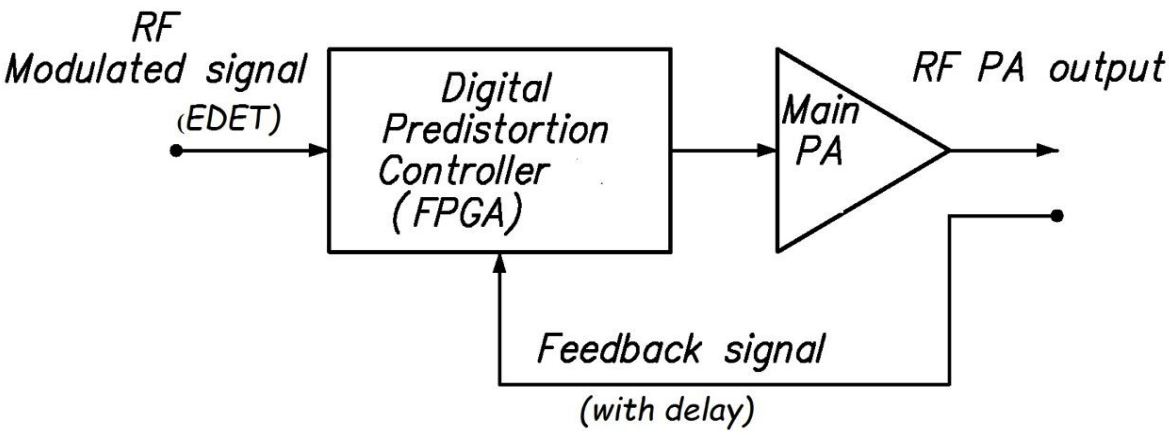

Figure 4.1 Hybrid DPD Technique implementation scheme.

4.3 System Description

The hybrid RF-DPD technique is a reformed form of DPD. It consists of mixed signal approach, which involves implementing the DPD in the form of an LUT on a FPGA/DSP platform. It works on indexed LUT entries, unlike raw I-Q data in order to apply appropriate correction parameters for the input signal at each instant as per the digital version of the instantaneous envelope power

of the modulated RF signal arranged in ascending order. The setup for the hybrid DPD system is described in the detailed block diagram of hybrid RF-DPD is shown in Fig. 4.2.

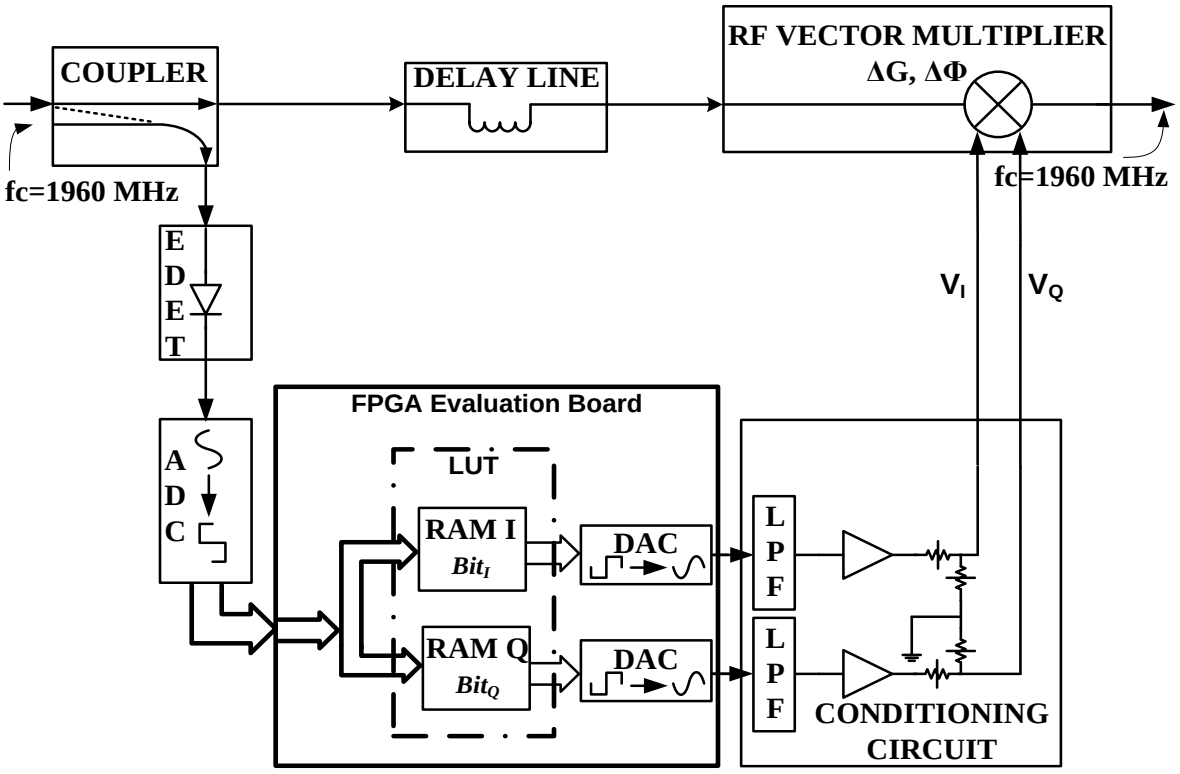

Figure 4.2 Block diagram of the hybrid RF-DPD system.

The input signal is fed from the Matlab/DSP Platform to the logarithmic envelope detector (EDET). EDET is used to determine the instantaneous power magnitude of the input modulated RF signal [56] and it passes only absolute values of the signal. The input signal is fed to the linear RF vector multiplier [57], at the same time, after passing through an RF delay line. The function of RF delay here is to provide a sufficient group delay to ensure that the RF signal and

corresponding correction signals are fed to the vector multiplier at the same time, so that the correction is applied to the signal envelope at the right instant of time.

The linear RF vector multiplier [57] shown in Fig. 4.2 adjusts the input RF signal's magnitude and phase through a multiplication by the correction parameters I_C and Q_C, stored in the LUT, which are implemented as random access memory (RAM) blocks in the FPGA. The LUT data is used to implement the PD function in the FPGA, which is generated from the characterization of the PA [49]. The hybrid DPD is implemented in two main steps: (a) characterizing the PA for generating an inverse nonlinear characteristic, and (b) implementing the PD function in the form of LUTs in the FPGA. The next section of this section discusses the PA characterization.

The following section covers the implementation of EMP model on FPGA along with its comparison with LUT model performance [13].

4.3.1 PA Characterization

The characterization is the prime step for successful implementation of hydrid-DPD technique. It involves retrieving the nonlinear complex gain characteristics of the PA. The characterization of the PA can performed under realistic 3G+ signals like WCDMA, Wi-Max and LTE [31] drive signals with an average power sufficiently high to drive the PA up to, but not beyond, its saturation power. WCDMA signals are used here for this purpose.

The PA characterization setup is shown in Fig. 4.3, where input and output samples are measured and can be stored for further processing to generate gain and phase information of their complex envelope by using a down-converter and a digital receiver.

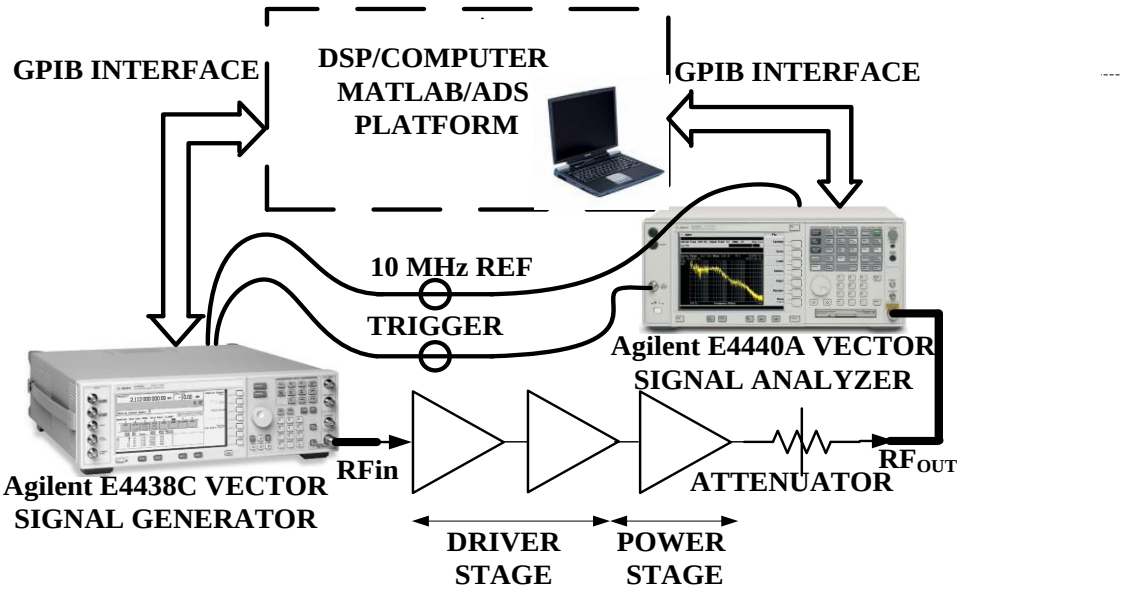

Figure 4.3 Setup for characterizing the power amplifier to obtain its nonlinear characteristics in terms of AM-AM and AM-PM responses.

The measurement setup consists of

- ✓ **Vector signal generator (VSG)**
- ✓ **Linear driver amplifier,**
- ✓ **Class AB PA ,1.96 GHz LDMOS**
- ✓ **Vector spectrum analyzer (VSA).**

The vector signal analyzer (VSA) or say spectrum analyzer by Agilent Technologies [58] as illustrated in Fig. 4.3 acts as digital receiver here. In this setup, the signal that we modulated and up-converted using signal generator, is pre-amplified by the driver amplifier in driver stage. The driver amplifier gain at input of the PA is about 30 dB. In power stage, the signal is amplified using Class AB PA.40 dB of attenuation is used at PA output. Class AB PA output is a distorted signal, depending upon the PA characteristics. The baseband I-Q data information of the input and

output signals are then used to derive the gain and phase response of the PA with respect to the input power termed as AM-AM and AM-PM responses, respectively. These characteristics are also described in Chapter 1 and are shown in Figure 2.2 and 2.3 respectively. The inverse nonlinear characteristics are generated in the DSP/computer for PA after getting amplitude and phase response of the given PA.

4.3.2 PD implementation

The PA linearization using hybrid DPD requires correct implementation of PD function, which has complex gain by characteristic nature. The required complex gain of the predistorter function should be converted to its rectangular coordinates to generate an LUT for implementation in an FPGA, so that it can be mapped to the required control voltages of the RF vector multiplier. This is shown in Figure 4.4.

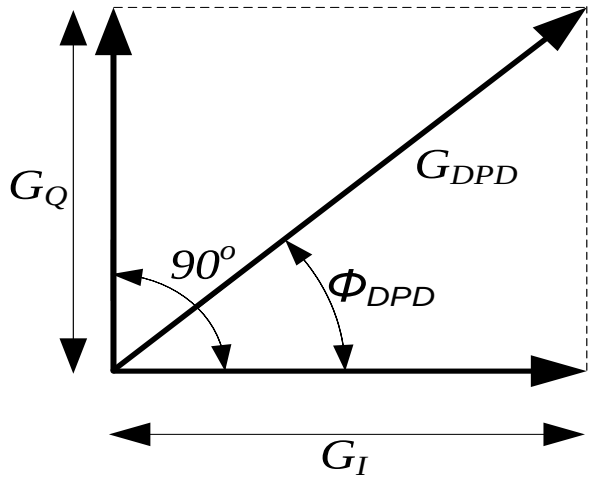

Figure 4.4 Vector decomposition of the predistorter complex gain characteristic for generating LUT entries corresponding to the control voltages of the RF vector multiplier with no I-Q imperfection.

If G_{DPD} and Φ_{DPD} are the respective gain and phase of the PD to be applied, then they can be represented in a rectangular form, from Figure 4.4, as

$$G_I = G_{DPD}\cos\left(\Phi_{DPD}\right) \tag{4.1}$$

$$G_Q = G_{DPD}\sin\left(\Phi_{DPD}\right) \tag{4.2}$$

where, G_I and G_Q are the respective I and Q components of this required complex gain characteristics of the PD.

Assuming a linear relationship between the linear gain components, they are converted into bits so that it can be stored in FPGA is form of LUT blocks.

This is given as

$$Bit_I = K_I G_I \tag{4.3}$$

$$Bit_Q = K_Q G_Q \tag{4.4}$$

where, K_I and K_Q are respective proportionality constants relating corresponding bits, Bit_I and Bit_Q, to their respective rectangular components, G_I and G_Q, of the PD complex gain.

The reference bit, Bit_{ref}, is determined that, when applied to both of the RAM blocks for the I and Q controls of the RF vector multiplier, to find K_I and K_Q. This results in unity gain of the RF path in the system. These equal bits correspond to equal control voltages (V_I and V_Q in Figure 4.2) at

the input pins of the RF vector multiplier; therefore, if there are no I-Q imperfections, the RF path of the system has a phase shift of 45° with respect to the phase of the system when only Bit_I is applied and with Bit_Q set to zero. Thus (4.3) and (4.4) can be written using these values of K_I and K_Q as

$$Bit_I = \frac{Bit_{ref} G_I}{\cos\left(45^\circ\right)} = Bit_{ref} G_I \sqrt{2} \tag{4.5}$$

$$Bit_Q = \frac{Bit_{ref} G_Q}{\sin\left(45^\circ\right)} = Bit_{ref} G_Q \sqrt{2} \tag{4.6}$$

The LUT entries obtained after the above mentioned methodology are in bit values which are sorted according to the ascending order of the bits, which correspond to the ascending order of the envelope power levels. The envelope power is converted into bit values using a linear relation between the digitized output voltage of the logarithmic detector and its input power (in dBm). The avoidance of sorting bits with respect to envelope power level can led to incorrect conversion of bits into digital output and, thus, is very important step to follow. The characterization of the logarithmic EDET is shown in Figure 4.5.

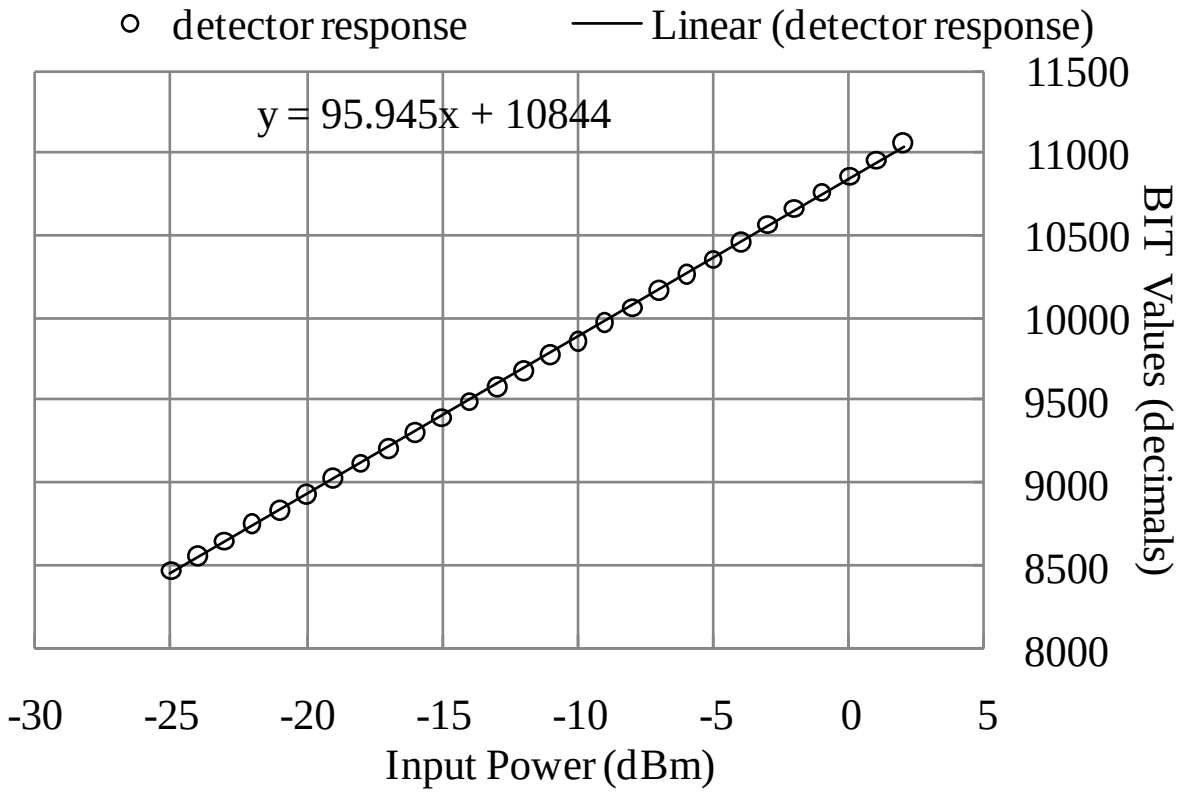

Figure 4.5 Linear response of logarithmic detector based on its characterization.

This characterization is carried out by sweeping the input RF power and reading the corresponding bit values by using the signal tap II logic analyzer feature of Quartus II software [13], [53].

4.4 I-Q imbalance Calibration

In ideal conditions, the in-phase (*I*) and quadrature-phase (*Q*) are orthogonal to each other, and the resultant, i.e. I-Q is at an angle of 45°. In general, both of the above-mentioned criterion are not fulfilled by I-Q data because of imperfection called as I-Q imperfections (as shown in figure). I-Q imperfections in the hybrid RF-DPD system may present in terms of quadrature imperfection,

where the control inputs are combined with a non-quadrature phase to give gain and phase correction by the RF vector multiplier, which is different from the actual gain and phase correction values required for the PD [53]. The other kind of imperfection may be an amplitude imbalance in the two paths of the control inputs from the digital-to-analog converters (DAC) of the FPGA to the control pins of the RF vector multiplier.

These imperfections can be reduced to a limited extent by tuning the gain of the conditioning circuit, as shown in Figure 4.2. However, this requires a precise tuning. Figure 4.6 shows the imperfect vector addition in the RF vector multiplier.

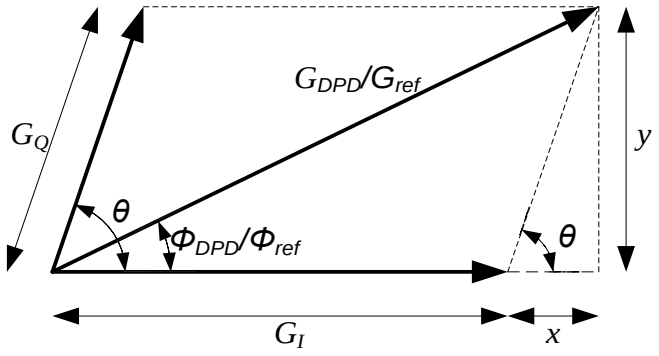

Figure 4.6 Vector decomposition of the predistorter complex gain characteristic for generating LUT entries corresponding to the control voltages.

The required complex gain characteristics of the predistortion function is decomposed into the respective I and Q components for the LUT to compensate for such imperfection in the LUT itself, according to the same imperfect vector addition. The new mapping coefficients, K_I and K_Q, are also generated accordingly. From Figure 4.6, the value of x and y are given by

$$y = G_{DPD} \sin\left(\Phi_{DPD}\right) \tag{4.7}$$

$$x = y\cot(\theta) \tag{4.8}$$

where θ is the quadrature imbalance, in vector multiplier and defined as the non-quadrature value with which the *I* and *Q* vectors combine to give the desired complex gain. The rectangular components of the required complex gain are now computed using (4.7), (4.8) and according to Figure 4.6 as

$$G_I = G_{DPD}\left(\cos\left(\Phi_{DPD}\right) - \sin\left(\Phi_{DPD}\right)\cot\theta\right) \tag{4.9}$$

$$G_Q = G_{DPD}\sin\left(\Phi_{DPD}\right)\mathrm{cosec}\left(\theta\right) \tag{4.11}$$

The proportionality constants, K_I and K_Q, are obtained and substituted in (4.3) and (4.4) which gives us

$$Bit_I = \frac{Bit_{ref}G_I}{\cos\left(\Phi_{ref}\right) - \sin\left(\Phi_{ref}\right)\cot\theta} \tag{4.12}$$

$$Bit_Q = \frac{Bit_{ref}G_Q}{\sin\left(\Phi_{ref}\right)\mathrm{cosec}\left(\theta\right)} \tag{4.13}$$

where, Φ_{ref} is the value of the relative phase of the system obtained when Bit_{ref} is applied to both I and Q RAMs simultaneously, with respect to the phase of the system when only Bit_I is applied, with Bit_Q set to zero. Φ_{ref} can be used to determine the I-Q amplitude imbalance in the system, if the value of Φ_{ref} is not exactly half of the value of θ. For such cases, using the measured value of Φ_{ref} in (4.9)-(4.10) results in unequal values of K_I and K_Q and compensates for the amplitude

imbalance. For an ideal case with no I-Q imperfection, θ and Φ_{ref} should be 90° and 45°, respectively, and (4.12)-(4.13) will reduce to the ideal case where the mapping is determined by (4.5)-(4.6).

4.5 Vector Multiplier characterization for I-Q imperfection

The other way for compensating I-Q imperfections is to characterize RF vector multiplier. The values θ and Φ_{ref} , discussed in previous section are the two parameters that characterize the I-Q imperfections in the RF-DPD system. These values can be solved and then used for adapting the LUT, as discussed in section 4.3.

Figure 4.7 describes the measurement setup for characterizing the hybrid RF-DPD system for I-Q imperfection.

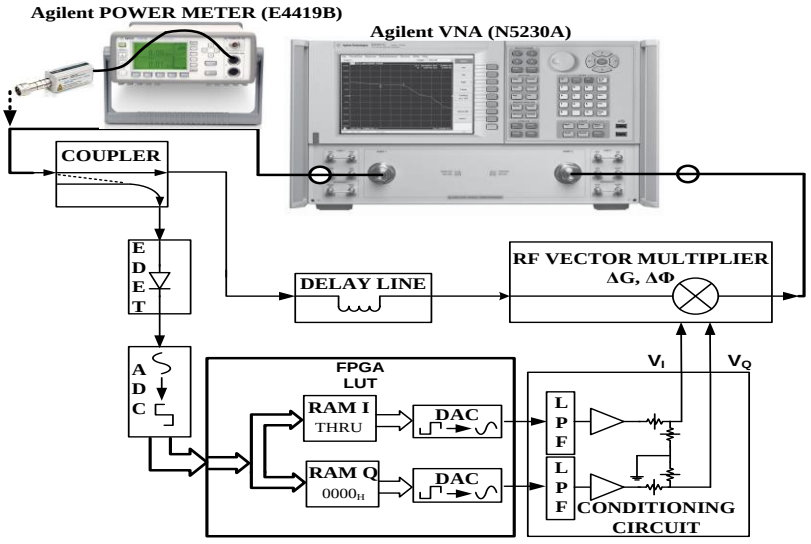

Figure 4.7 Setup for characterizing the RF vector multiplier for I-Q imperfection in the hybrid RF-DPD system.

The vector network analyzer (VNA) is operated in power sweep mode with a thru-response calibration. This setup and method is similar to a typical setup for measuring AM/PM characteristics of a nonlinear system [27]. This characterization involves steps to find the absolute phase of I and Q axes used by the RF vector multiplier for vector addition. The tricky method behind this is the varying of only one of the control inputs of the RF vector multiplier, while keeping the other at a nominal voltage value.

The phase of the RF path is measured with the VNA operating in a linear power sweep mode with different entries in the RAM tables. Depending upon the RAM entries inside the FPGA, the RF vector multiplier's control voltages sweep corresponding to the input power sweep. This left us with three cases for which phase of the RF path is measured, as shown in Table 4.1.

Table 4.1 Different cases in the characterization of the RF vector multiplier in the hybrid RF-DPD system

Case	RAM I	RAM Q	Comment
I	*THRU*	*ZERO*	Determines absolute phase of I-axis
II	*ZERO*	*THRU*	Determines absolute phase of Q-axis
III	*THRU*	*THRU*	Determines IQ axis and hence Φ_{ref} to obtain I-Q amplitude imbalance

THRU represents when all the RAM entries are the bits arranged in their ascending order, and the control voltage at the input of the RF vector multiplier sweeps in the fashion as the RF power sweep at the input of the EDET [59].

On the other hand, *ZERO* represents when all the bit entries of the RAM are initialized to zero hexadecimal values. For this condition, the control voltage is fixed to the nominal value and does not vary with the input RF power. These different bit-values are loaded in the RAM by initializing it using the corresponding memory initialization files (MIF).

The absolute phase plots of these cases in polar representation are shown in Figure 4.8

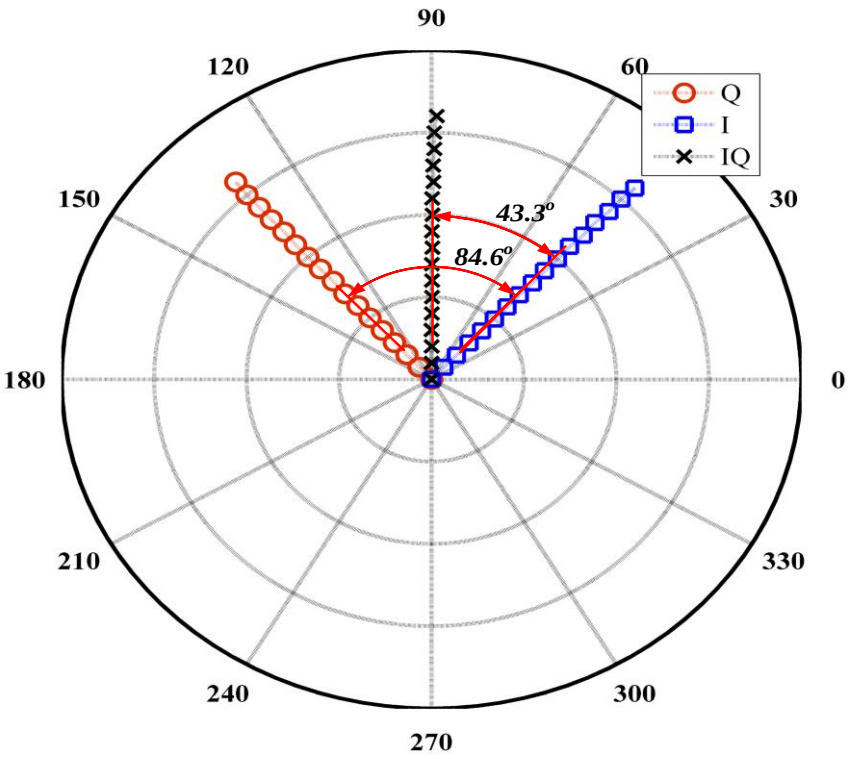

Figure 4.8 Absolute phase measurement of different cases in RF vector multiplier characterization.

The imperfection measure here is denoted by the term θ, which is obtained by subtracting the absolute phase of the I-axis (case I) from the absolute phase of the Q-axis (case II). The value of

Φ_{ref} is obtained by subtracting the absolute phase of the I-axis (case I) from the absolute phase of the I-Q plot (case III). From Fig. 4.8, the θ and Φ_{ref} are approximately 84.6° and 43.3°, respectively.

Although, the proposed characterization and compensation methodology for hybrid RF-DPD is independent of the dynamic behaviour of the PA, the LUT based method implemented here, compensates for static nonlinearity using indirect learning method based on the open loop characterization of PA. The proposed compensation remains intact, if the characteristics of the PA change and the LUT is updated to maintain the performance of predistorter, with no need to compute new mapping coefficients, K_I and K_Q. The system used here is made adaptive to compensate for the dynamic behavior of the PA, as discussed in [49],[13],[53],[27], but still an additional adaptive loop is necessary for hybrid RF-DPD to adapt to the changing I-Q imperfections with the process, voltage and temperature, with can affect the calibration as well as compensation of the system.

Table 4.2 represents the measured ACLR performance at ±3 MHz offset from the center of the main and offset carrier for one- and three-carrier WCDMA signals, respectively. It shows the Lower Value as well as upper values of ACLR for both single-carrier and three-carrier WCDMA signals. An improvement of ~ 2 dB in terms of ACLR is observed with implementation of I-Q compensation.

However, the correction here is limited due to the memory effect present in the amplifier, which cannot be compensated using the static LUT based predistortion model.

Table 4.2 Measured ACLR summary of various conditions for one- and three-carrier WCDMA signals.

Contents		RF-DPD OFF	RF-DPD ON No Compensation	RF-DPD ON With Compensation
ACLR (dBc) Lower/ Upper	One-Carrier	-37.9/ -37.2	-48.5/-48.1	-50.3/-52.8
	Three-Carrier	-38.5/-39.0	-47.6/-45.1	-48.9/-47.3

4.6 Envelope Memory Polynomial for memory effect inclusion

In most of the FPGA implementation for MP model was the first option to be implemented in FPGA, but because of its non-absolute characteristic (4.14), it is impossible to be used it at the input of the FPGA.

The EDET in the input block of the FPGA allows only absolute termed data to pass through it and thus prohibit the use of MP model [10] (discussed in chapter 3, section 3.2) for DPD implementation.

$$y_{MPM}(n) = \sum_{k=1}^{K}\sum_{m=0}^{M} a_{km}\, x(n-m)\left|x(n-m)\right|^{k-1} \tag{4.14}$$

where k is non-linearity order m is memory depth.

Therefore EMP model is studied an alternative to include memory effects, as it is capable of providing absolute value input (4.15) to the EDET of the FPGA.

$$y_{EMPM}(n) = \sum_{k=1}^{K}\sum_{m=0}^{M} a_{km}\, x(n)\left|x(n-m)\right|^{k-1} \tag{4.15}$$

where k is non-linearity order m is memory depth.

The EMP model is different from MP model in terms of its characteristics .MP has $x(n-i)$ as input which means it is part of the matrix system and is not an absolute value while in EMP Model, $x(n)$ acts as an independent and thus absolute value, which makes EMP model , the absolute one and thus perfect to be used in FPGA implementation.

The EMP model assumes that memory effects mostly arise due to delayed envelope of the signal, and phase of delayed signals have less impact on the model performance. Similar to memory polynomial model, the coefficients of EMP model can also be calculated using least squares method.

Figure 4.9 shows the block diagram of EMP model and it can be observed that complex gain can be calculated as sum of many absolute gain branches.

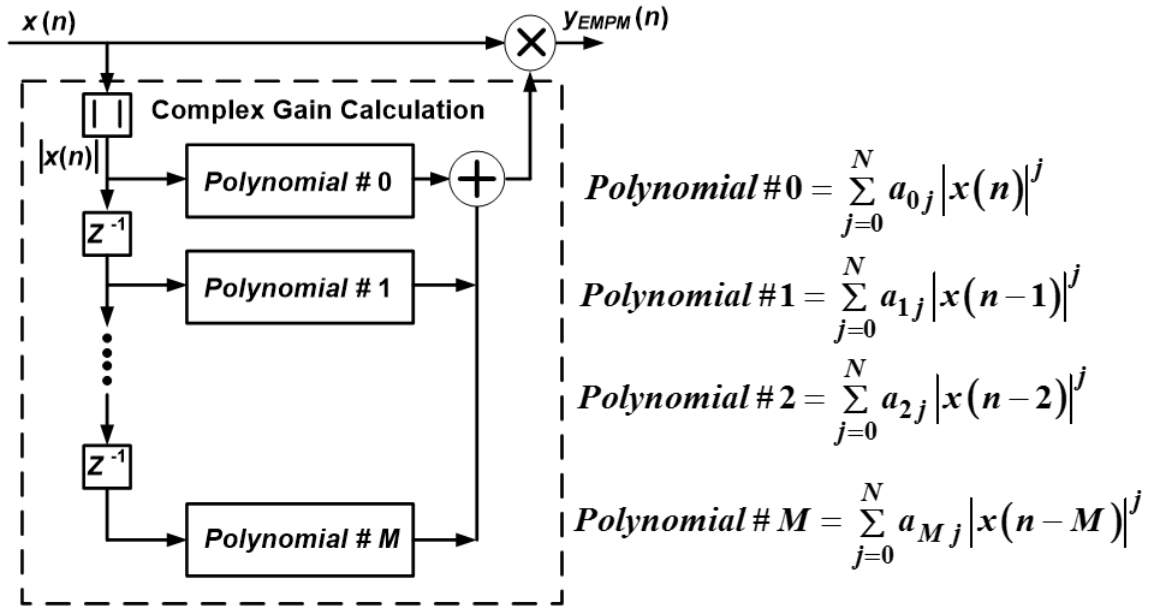

Figure 4.9 Detailed block diagram of EMP model

Similar to LUT, these branches can be implemented in FPGA individually and their sum can be provided as a system gain to the vector multiplier.

The linearization performance of EMP model is validated with a class AB PA, with respect to memory polynomial and LUT based models. The PA is characterized with single and multi-carrier 3G WCDMA signals with PAPR of 10.5 dB.

The results from Figure 4.10 shows an improvement of approximately 2 dB in EMP model as compared to LUT model, without DPD, which still left scope for better trade-offs of EMP model over LUT with DPD implementation

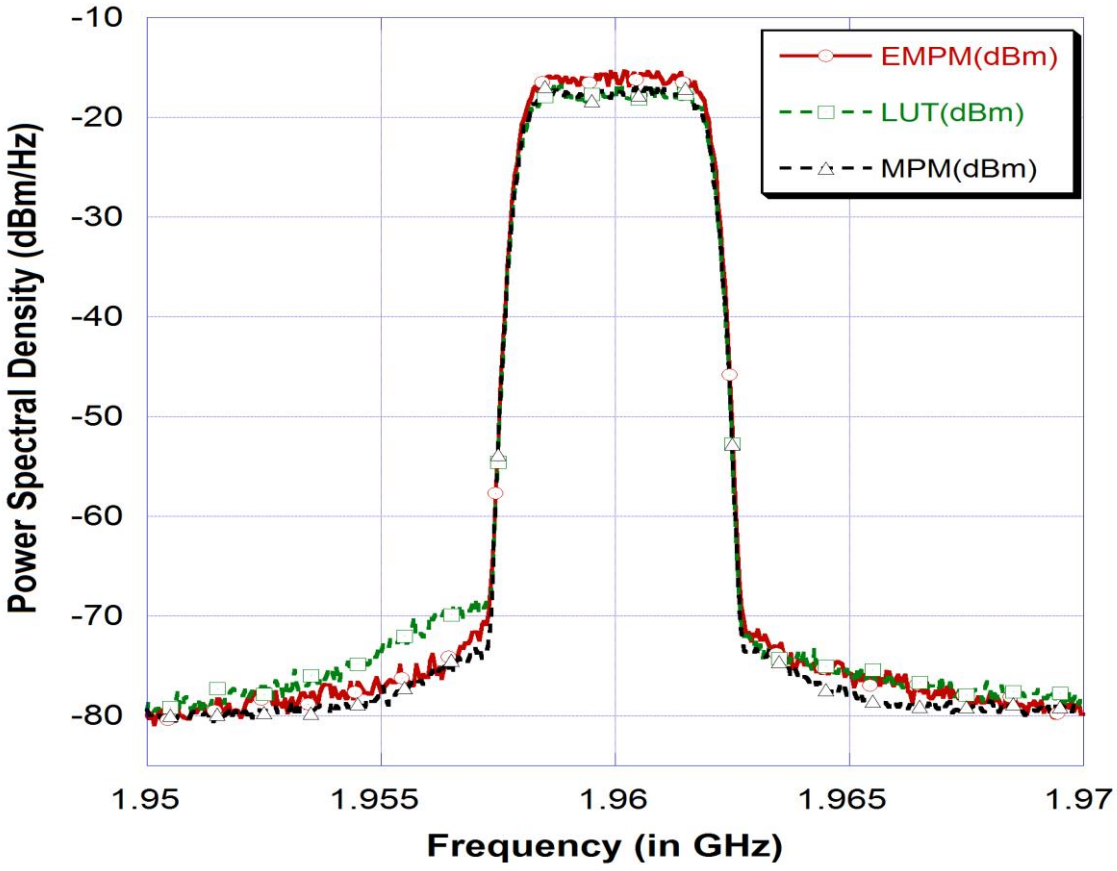

Figure 4.10 Measured output spectrum of the PA for one-carrier WCDMA signal.

4.7 Conclusion

A hybrid-RF DPD system implementation system is studied. Various components to be used, such as an envelope detector and a vector multiplier, are calibrated to provide proper implementation conditions. I/Q imbalance calibration steps are carried out, which provided 2-3 dB improvements in LUT based PD implementation. An envelope memory polynomial based DPD implementation is carried out to assess its usefulness in comparison to LUT based implementation and the EMP model is observed to be able to compensate for memory effects in DPD application.

Chapter Five: Summary and Future plans

5.1 Summary

This thesis is devoted to the study of alternative models for high power amplifier modeling and their application in digital/hybrid pre-distortion. The main contributions of the thesis can be summarized as follows:

1. A Pseudo-Zernike polynomial based approach is investigated for signals with non-uniform power spectrum density functions, which provides less coefficient dispersion for ease of implementation of DPD model. Proposed model can replace orthogonal polynomial for similar complexity.
2. A 2-step rational function model had been proposed for more accurate forward and inverse modeling performances. The model approximates recursive nature of the rational polynomial presentation. However, while other recursive models suffer from stability problems, proposed model allows operation in open loop mode. This provides better in-band and out-of-band modeling performance.
3. An hybrid (RF/digital) predistortion scheme is studied for complete RF-in and RF-out system. Such systems are useful for the manufacturer of the PA, who wants to implement PA predistortion, but do not have access to digital domain of SDR system. Previously, LUT based memoryless nonlinear characterization is used in hybrid DPD systems. However, in this thesis envelope polynomial is used for memory effect correction along with the nonlinearity correction.

5.2 Key Points for Future Developments

Based on the results achieved in this thesis, the natural extension of the work in future can be as follows:

- Implementation of 2-step rational function model for DPD application.
- Analyze the trade-offs of using EMP model in comparison to LUT based methods.
- Implementing EMP model in existing FPGA platform of hybrid RF-DPD to compensate for memory effects.
- Extension of 2-step rational function model for multi-band non-linear amplifiers.
- Extension of FPGA based platform of hybrid RF-DPD for concurrent multi-band applications.

References

[1] D. Theckedath and T. J. Thomas, "The 700 MHz Spectrum Auction," *Hillnotes, Industry, infrastructure and Resource Division.*

[2] M. Rawat, "Artificial Neural Networks for Behavioral Modeling and Digital Predistortion for Software Defined Transmitters", *Thesis,* Sep. 2012

[3] Brian Jackson, "Canadians to consume 800% more mobile data by 2018," *Cis*co, *itbusiness.ca, Technology Division.*

[4] Matt Gillies, "Canadian Mobile Data Usage on the Rise, Inspiring Innovation for Service Providers", *Cisco, Cisco Canada Blog.*

[5] http://www.ericsson.com/us/ourportfolio/products/wcdma-radio-access-network

[6] http://www.agilent.ca/about/newsroom/tmnews/background/wimax/

[7] http://www.enensys.com/technologies/dvb-t-overview.html

[8] http://www.home.agilent.com/agilent/editorial.jspx?ckey=1803101&id=1803101&lc=eng&cc=CA

[9] J. C. Pedro and S. A. Maas, "A comparative overview of microwave and wireless power amplifier behavioral modeling approaches," IEEE Trans. Microw. Theory Tech., vol. 53, no. 4, pp. 1150–1163, Apr. 2005.

[10] M.Rawat, K.Rawat and Fadhel M. Ghannouchi, "Three-Layered Biased Memory Polynomial for Dynamic Modeling and Predistortion of Transmitters With Memory," IEEE Trans. on Circuit and Systems, vol.60, no.3, pp. 768-777, March 2013

[11] M.V. Amiri, S.A. Bassam, M.Helaoui and Fadhel M. Ghannouchi, "Estimation of crossover DPD using orthogonal polynomials in fixed point arithmetic," AEU - International Journal of Electronics and Communications, 2013 Accepted

[12] ADL5390 RF/IF Vector Multiplier, Analog Devices, Norwood, MA 02062-9106, USA, 2004.

[13] K. Rawat, M. Rawat, and F.M. Ghannouchi, "Compensating I-Q Imperfections in Hybrid RF/Digital Predistortion with Adapted Look up Table Implemented in FPGA," IEEE Trans. on Circuits and Systems II, vol. 57, no. 5, pp. 389-393, May 2010.

[14] J.K. Cavers, "Adaptation Behavior of a Feedforward Amplifier Linearizer", IEEE Transactions on Vehicular Technology, vol. 44, no. 1, pp. 31-40, Feb. 1995.

[15] T. Arthanayake, H.B. Wood, "Linear Amplification Using Envelope Feedback", IEEE Electronic Letters, vol. 7, no. 7, pp. 145-146, April 1971.

[16] J. Cardinal, F.M. Ghannouchi, "A New Adaptive Double Envelope Feedback (ADEF) Linearizer for Solid State Power Amplifiers", IEEE Transactions on Microwave Theory and Techniques, vol. 43, no. 7, pp. 1508-1515, July 1995.

[17] S.C. Cripps, RF Power Amplifiers for Wireless Communications, Boston, MA: Artech House, 1999.

[18] H.S. Black, "Translating System", U.S. Patent 1,686,792, filed 3 Feb. 1925, granted 9 Oct. 1928.

[19] H.S. Black, "Stabilised Feedback Amplifiers", The Bell System Technical Journal, vol. 13. no. 1, pp. 1-18, Jan. 1934.

[20] H.S. Black, "Wave Translation System", U.S. Patent 2,102,671, filed 22 Apr. 1932, granted 21 Dec. 1937.

[21] J. Yi, Y. Yang, M. Park, W. Kang, B. Kim, "Analog Predistortion Linearizer for High-Power RF Amplifiers", IEEE Transactions on Microwave Theory and Techniques, vol. 48, no. 12, pp. 2709-2713, Dec. 2000.

[22] M.D. Benedetto, P. Mandarini, “A New Analog Predistortion Criterion with Application to High Efficiency Digital Radio Links”, IEEE Transactions on Microwave Theory and Techniques, vol.43, no.12, pp. 2966-2974, Dec. 1995.

[23] Y. Kim, I. Chang, Y. Jeong, “An Analog Predistortion Linearizer Design”, Microwave Journal, vol. 48, no. 2, pp. 118-126, Feb. 2005

[24] J. Yi, Y. Yang, M. Park, W. Kang, B. Kim, “Analog Predistortion Linearizer for High-Power RF Amplifiers”, IEEE Transactions on Microwave Theory and Techniques, vol. 48, no. 12, pp. 2709-2713, Dec. 2000.

[25] S. Boumaiza, J. Li, F.M. Ghannouchi, “Implementation of an Adaptive Digital/RF Predistorter using direct LUT synthesis”, in 2004 IEEE International Microwave Symposium MTT-S., pp. 681-684.

[26] S. Boumaiza, J. Li,M. Jaidane-Saidane, and F.M. Ghannouchi, “Adaptive digital/RF predistortion using a nonuniform LUT indexing function with built-in dependence on the amplifier nonlinearity,” IEEE Trans. Microw. Theory Tech., vol. 52, no. 12, pp. 2670–2677, Dec. 2004.

[27] E. G. Jeckeln, F. Beauregard, M. A. Sawan, and F. M. Ghannouchi, "Adaptive Baseband/RF Predistorter for Power Amplifiers Through Instantaneous AM-AM and AM-PM Characterization using Digital Receivers," IEEE MTT-S Int. Microwave Symp. Dig., vol. 1, pp. 489-492, May 2000.

[28] Wangmyong Woo, M. D. Miller, J. S Kenney, “A Hybrid Digital/RF envelope predistortion linearization system for power amplifiers”, IEEE Trans. Microw. Theory and Tech., vol. 53, no. 1, pp. 229-237, Jan 2005.

[29] R. Sweeney, “Practical Magic,” IEEE Microw. Magazine, vol. 9, no. 2, pp. 73–82, Apr. 2008.

[30] B. Kim, I. Kim, J. Moon, “Advanced Doherty Architecture,” IEEE Microw. Magazine, vol. 11, no. 5, pp. 72–86, Aug. 2010.

[31] Piyush Rawat, Meenakshi Rawat and Fadhel M. Ghannouchi, “Pseudo-Zernike Polynomials for numerically stable PA modeling using 3G+ signals”, *MOTL-Microwave Optical Technology Letter, 2014 Accepted.*

[32] M. Rawat, K. Rawat, F. M. Ghannouchi, S. Bhattacharjee, and H. Leung, "Generalized Rational Functions for Reduced-Complexity Behavioral Modeling and Digital Predistortion of Broadband Wireless Transmitters," *IEEE Transactions on Instrumentation and Measurement*(online).

[33] M. Aziz, M. Rawat, and F. M. Ghannouchi, "Rational Function Based Model for the Joint Mitigation of I/Q Imbalance and PA Nonlinearity," *IEEE Microwave and Wireless Components Letters*, vol. 23, no. 4, pp. 196-198, April 2013.

[34] J. I. Díaz, C. Pantaleón, I. Santamaría, T. Fernández and D. Martínez, “Nonlinearity estimation in power amplifiers based on subsampled temporal data,” *IEEE Trans. Instrum. Meas.*, vol. 50, no. 4, pp. 882–886, Aug. 2001.

[35] M. Rawat and F. M. Ghannouchi, “Distributed Spatiotemporal Neural Network for Nonlinear Dynamic Transmitter Modeling and Adaptive Digital Predistortion,” *IEEE Trans. Instrum. Meas.*, vol. 61, no. 3, pp. 595 - 608, Nov. 2011.

[36] Lei Ding, G. T. Zhou, D. R. Morgan, Ma Zhengxiang, J. S. Kenney, Kim Jaehyeong and C. R. Giardina, "A robust digital baseband predistorter constructed using memory polynomials," *IEEE Trans. on Communications*, vol. 52, no.1, pp. 159–165, Jan. 2004.

[37] R. Raich, H. Qian, and G. T. Zhou, "Orthogonal polynomials for power amplifier modeling and predistorter design," *IEEE Trans. Veh.Technol*., vol. 53, no. 5, pp. 1468–1479, Sep. 2004.

[38] C. Jebali, N. Boulejfen, M. Rawat, A. Gharsallah and F. M. Ghannouchi, "Modeling of Wideband RF Power Amplifiers Using Zernike Polynomials," *Wiley International Journal of RF and Microwave Computer-Aided Engineering*, 2011 Accepted.

[39] A.B. Bhatia and E. Wolf, "On the circle polynomials of Zernike and related orthogonal sets," *Proc Philosophical Society of Cambridge*, vol. 50, pp. 40-48, 1954.

[40] D. R. Morgan, M. Zhenngxiang, L. Kim, M. G. Zierdt, and I. Pastalan, "A generalized memory polynomial model for digital predistortion of RF power amplifiers," *IEEE Trans. Signal Process.*, vol. 54, no. 10, pp. 3852–3860, Oct. 2006.

[41] S. Boumaiza, M. Helaoui, O. Hammi, T. Liu, and F. M. Ghannouchi, "Systematic and adaptive characterization approach for behavior modeling and correction of dynamic nonlinear transmitters," *IEEE Trans. Instrum. Meas.*, vol. 56, no. 6, pp. 2203–2210, Dec. 2007.

[42] M. Rawat, K. Rawat, and F. M. Ghannouchi, "Adaptive digital predistortion of wireless power amplifiers/transmitters using dynamic real-valued focused time-delay line neural networks," *IEEE Trans. Microw. Theory Tech*., vol. 58, no. 1, pp. 95–104, Jan. 2010.

[43] T. M. Cunha, P. M. Lavrador, E. G. Lima, and J. C. Pedro, "Rational function-based model with memory for power amplifier behavioral modeling," in *Proc. Workshop INMMIC*, Apr. 2011, pp. 1–4.

[44] S. A. Bassam, M. Helaoui, and F. M. Ghannouchi, ”2-D digital predistortion (2-D-DPD) architecture for concurrent dual-band transmitters,”IEEE Trans. Microwave Theory & Tech., vol. 59, no. 10, pp. 2547-2553, Oct.2011.

[45] T. R. Cunha, E. G. Lima, H. M. Teixeira, P. M. Cabral, and J. C. Pedro, ”A new predistorter model based on power amplifier physical knowledge”, in Proc. Workshop on Integrated Nonlinear Microwave and Millimetre- Wave Circuits.,Apr. 2010, pp.140-143.

[46] E. Ngoya, C. Quindroit and J.M. Nebus, ”On the continuous-time model for nonlinear-memory modeling of RF power amplifiers, IEEE Trans. Microwave Theory & Tech., vol. 57, no. 12, pp. 3278-3292, Dec. 2009.

[47]] D. Ronnow, D. Wisell, and M. Isaksson, “Three-tone characteriza- tion of nonlinear memory effects in radio-frequency power ampli- fiers,” *IEEE Trans. Instrum. Meas.*, vol. 56, no. 6, pp. 2646–2657, Dec. 2007.

[48] O. Hammi and F. M. Ghannouchi, "Twin Nonlinear Two-Box Models for Power Amplifiers and Transmitters Exhibiting Memory Effects With Application to Digital Predistortion," *IEEE Microwave and Wireless Components Letters*, vol. 19, no. 8, pp. 530-532, Aug. 2009.

[49]] W. Woo, M. D. Miller, J. S. Kenney, “A Hybrid Digital/RF Envelope Predistortion Linearization System for Power Amplifiers,” IEEE Trans. Microwave Theory and Techniques, vol. 53, no.1, pp. 229-237, Jan. 2005.

[50] http://www.altera.com/products/fpga.html

[51] http://en.wikipedia.org/wiki/Digital_signal_processing

[52] J.K. Cavers, “Amplifier linearization using a digital predistorter with fast adaptation and low memory requirements,” IEEE Trans. Veh. Technol., vol. 39, pp. 374-382, Nov. 1990.

[53] K. Rawat, O. Hammi, F. M. Ghannouchi, “Investigating effects of quadrature imperfection of vector multiplier in implementing RF/digital predistortion,” presented at the 10th annual IEEE Wireless and Microwave Technology Conference WAMICON, Clearwater, FL, Apr. 20-21, 2009, Paper 1569164269.

[54] H. B. Nasr, S. Boumaiza, M. Helaoui, A. Ghazel, F. M. Ghannouchi, “On the critical issues of DSP/FPGA mixed digital predistorter implementation,” in Proc. IEEE Asia-Pacific Conf., Dec. 2005.

[55] Altera Application Note AN-314-1.0 Digital predistortion reference design, Altera Corporation Inc., San Jose, CA, July 2003.

[56] AD8313 Logarithmic detector/ controller data sheet, Analog Devices Inc., Norwood, MA, USA, 2004.

[57] MAX2045/MAX2046/MAX2047 High gain vector multipliers data sheet, Maxim Integrated Products, Inc., Sunnyvale, CA.

[58] Altera EP1S80 DSP development board data sheet, Altera Corporation Inc., San Jose, CA, Dec. 2004.

[59] Agilent PNA Application Note AN1408-10, Agilent Technologies Inc., Santa Clara, CA, USA.

[60] C. Knapp, G. Carter, "The generalized correlation method for estimation of time delay," IEEE Transactions on Acoustics Speech and Signal Processing, vol. 24(4), pp. 320-327, 1976.

[61] Hazem M. El-Bakry, and Qiangfu Zhao, “Fast Sub-Matrix Detection Using Neural Networks and Cross Correlation in the Frequency Domain,” Second Workshop of Tohoku

Branch, IPSJ, (Information Processing Society of Japan), University of Aizu, Aizuwakamatsu, Japan, Jan. 21, 2005